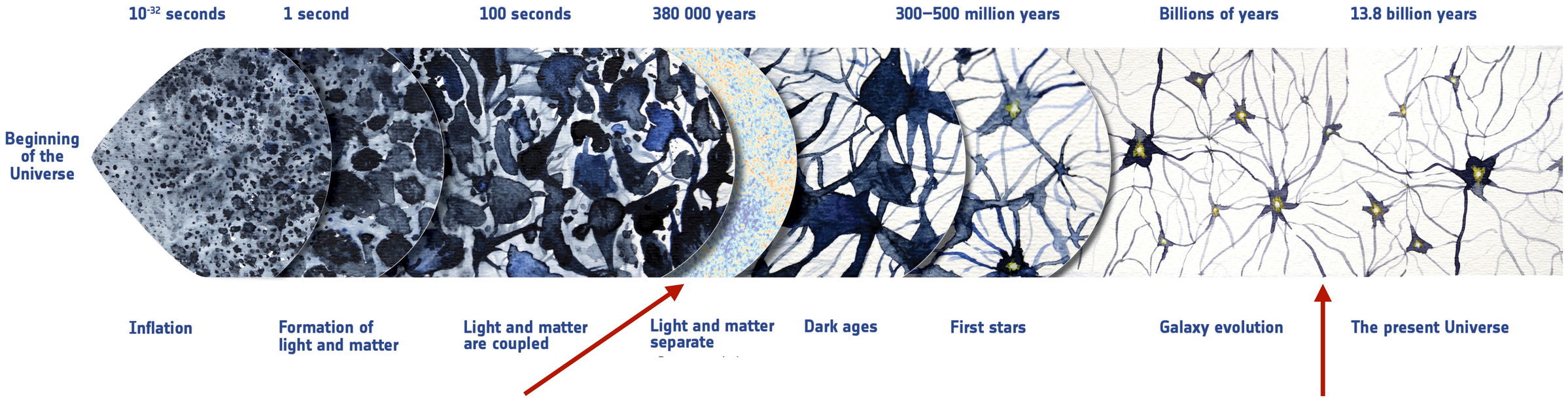
Probing high-redshift structure growth: forecasts and first insights from Euclid AGNs × CMB Lensing Cross-Correlations

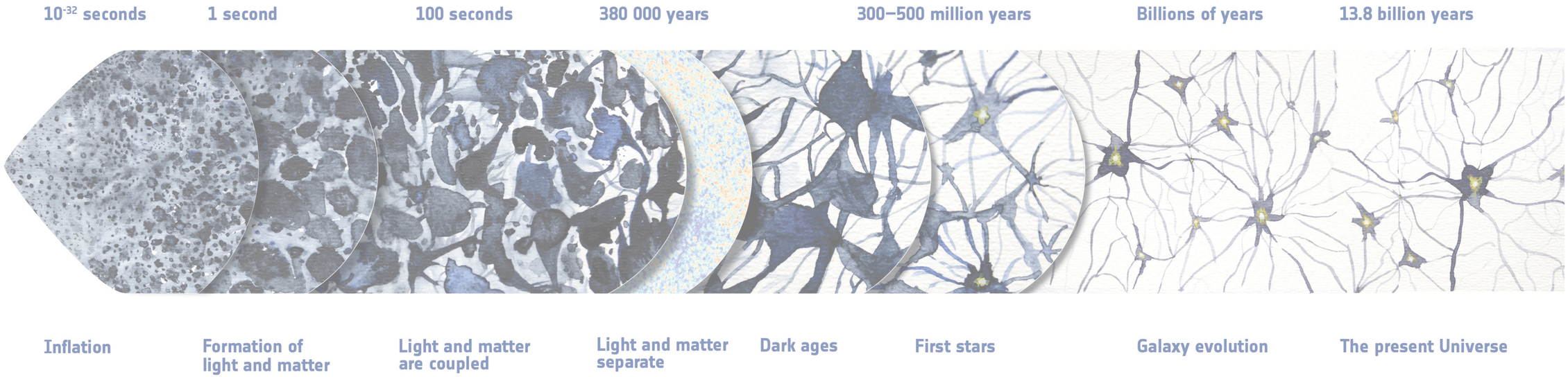
Matteo Peronaci, Giulia Piccirilli, Marina Migliaccio, Giulio Fabbian

"29th International Conference on Particle Physics & Cosmology"
Leiden – August 25, 2026

Cosmic history and scientific targets



Cosmic history and scientific targets



early time universe → **late time universe**

primordial non-Gaussianity from scale-dependent bias

$$f_{\mathrm{NL}}$$

amplitude of matter perturbations at different redshifts

$$\sigma_8(z)$$

dark energy e.o.s and density parameter

$$w_0\,,\ \Omega_\Lambda^0$$

Observables – LSS tracer

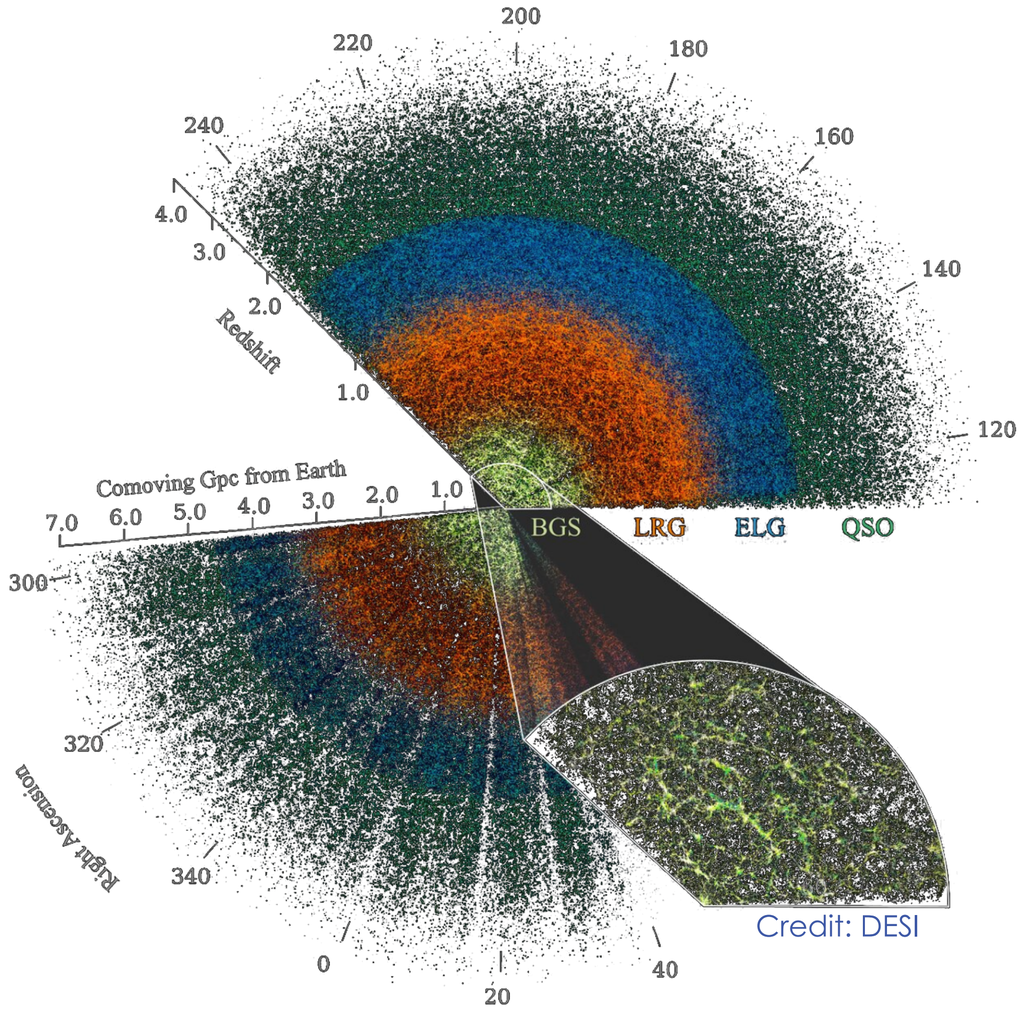
Active Galactic Nuclei !

Why AGNs?

Brighter, more massive, less affected by dust
⟶ can be observed up to $z \gtrsim 5$

Trace the same dark matter potential wells that host galaxy formation

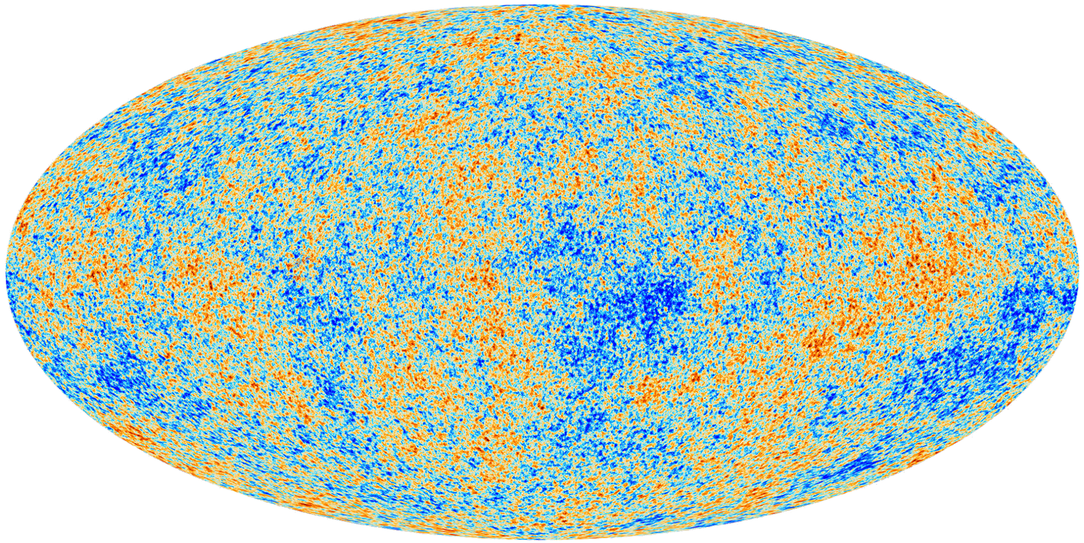
Highly biased sources



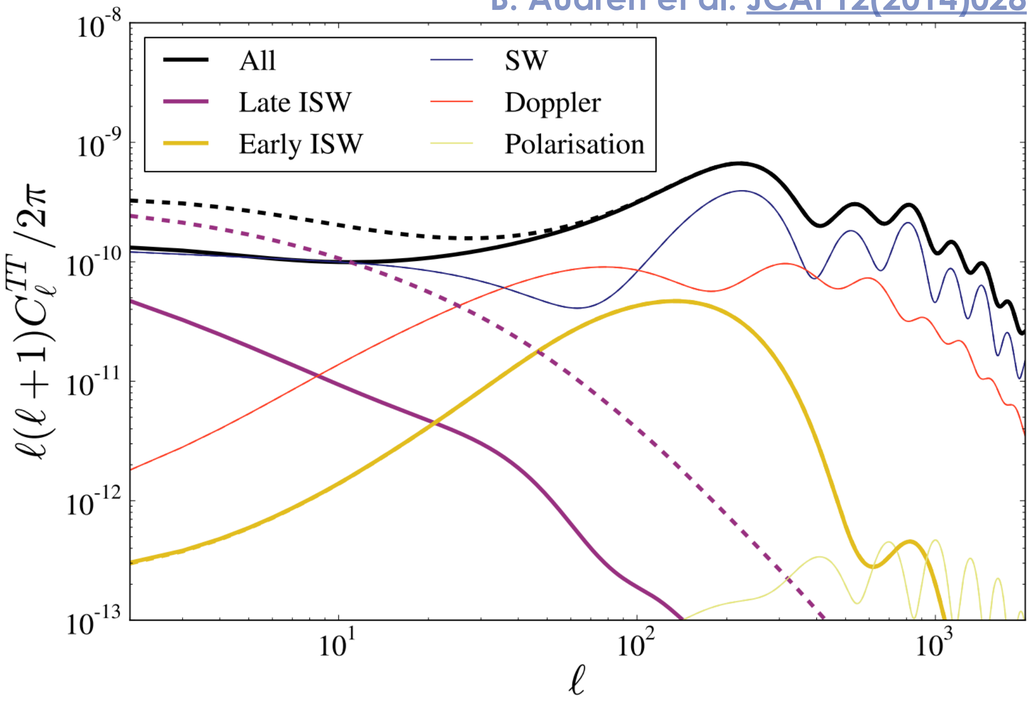
Observables – CMB temperature anisotropies

Primordial perturbations at $z \approx 1100$

Secondary anisotropies imprinted along the way
⟶ late-time Integrated Sachs-Wolfe effect



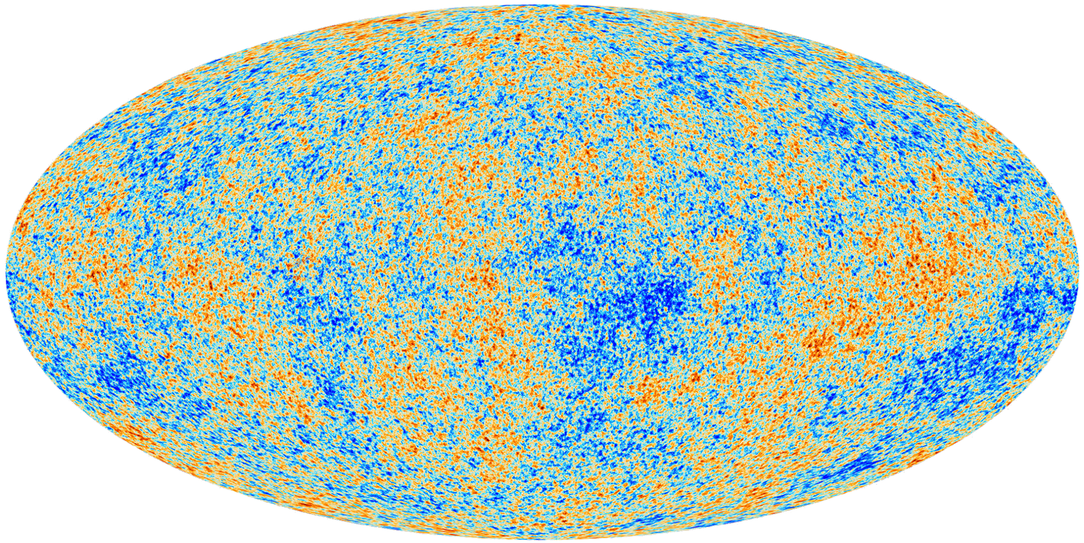
B. Audren et al. JCAP12(2014)028



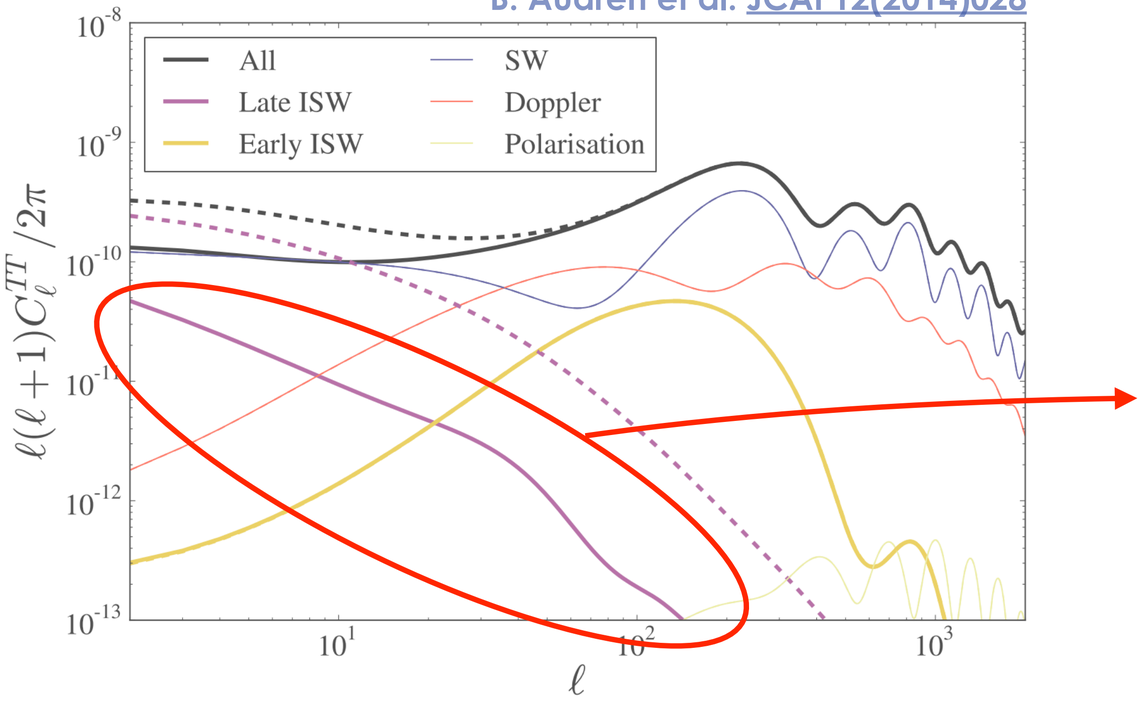
Observables – CMB temperature anisotropies

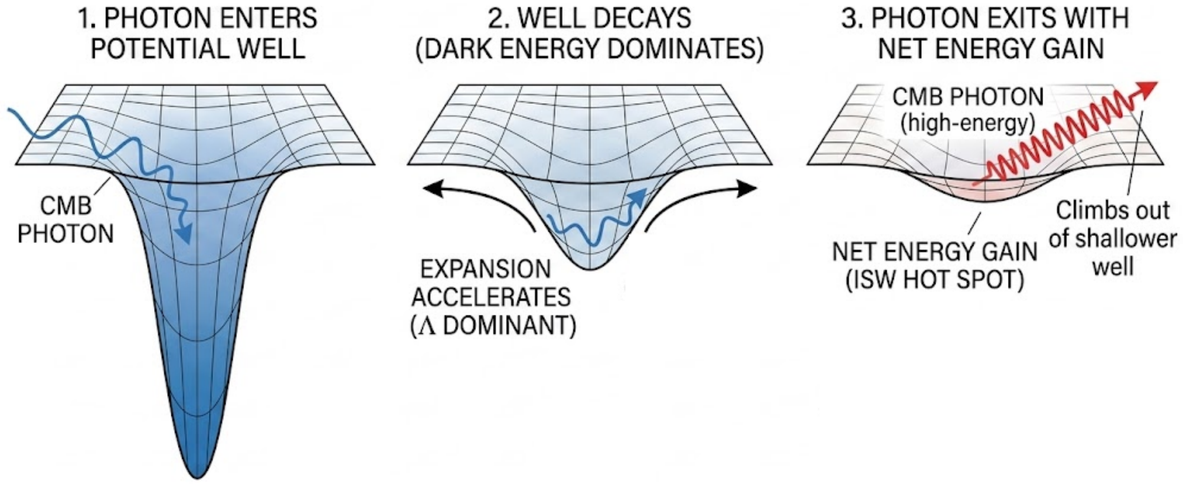
Primordial perturbations at $z \approx 1100$

Secondary anisotropies imprinted along the way
⟶ late-time Integrated Sachs-Wolfe effect



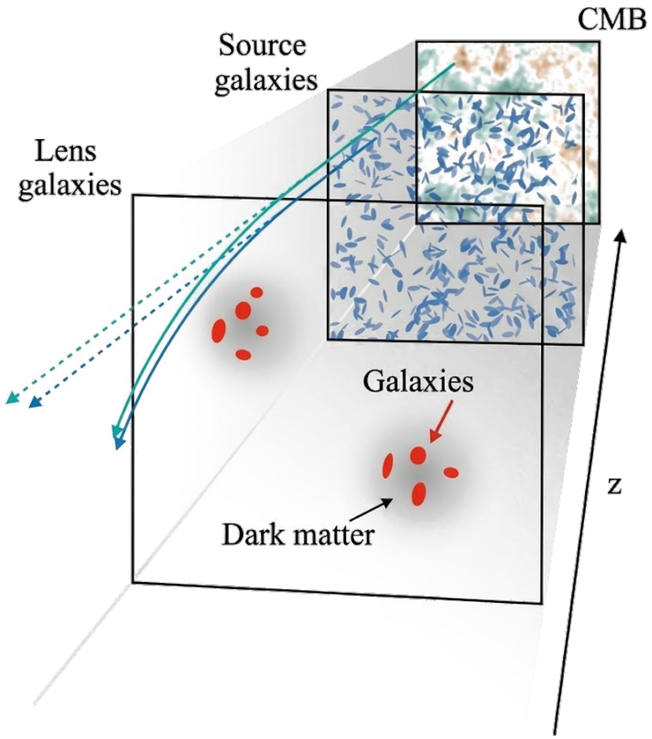
B. Audren et al. JCAP12(2014)028



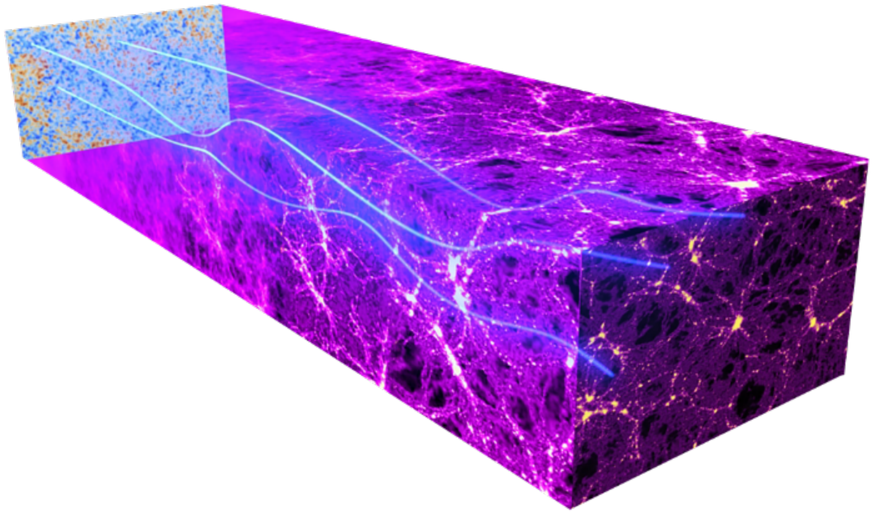


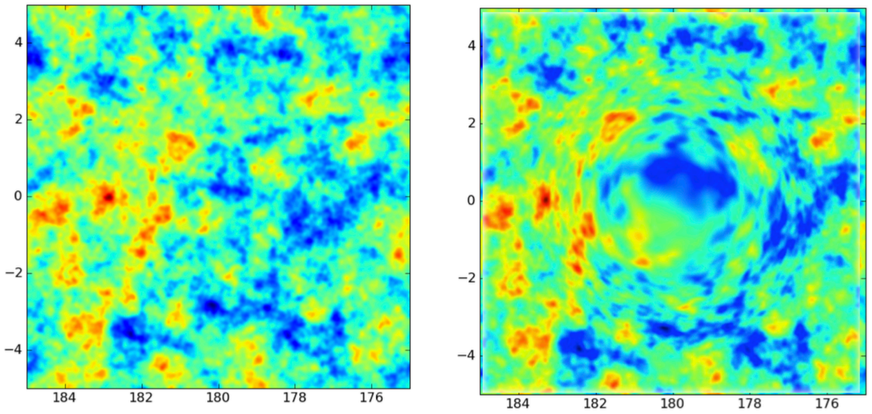
Observables – CMB lensing

LSS deflects the CMB photons along the whole line of sight



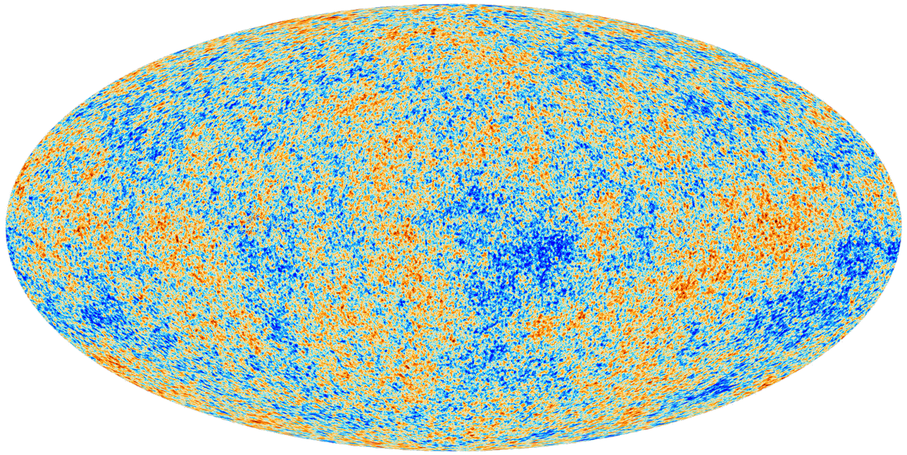
With a resulting deflection of photon geodesics



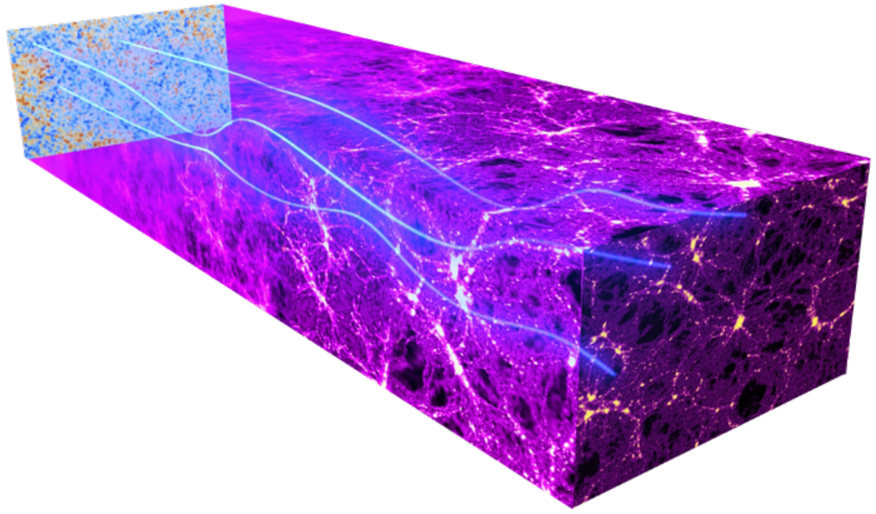


unlensed **lensed**

Cross-correlations

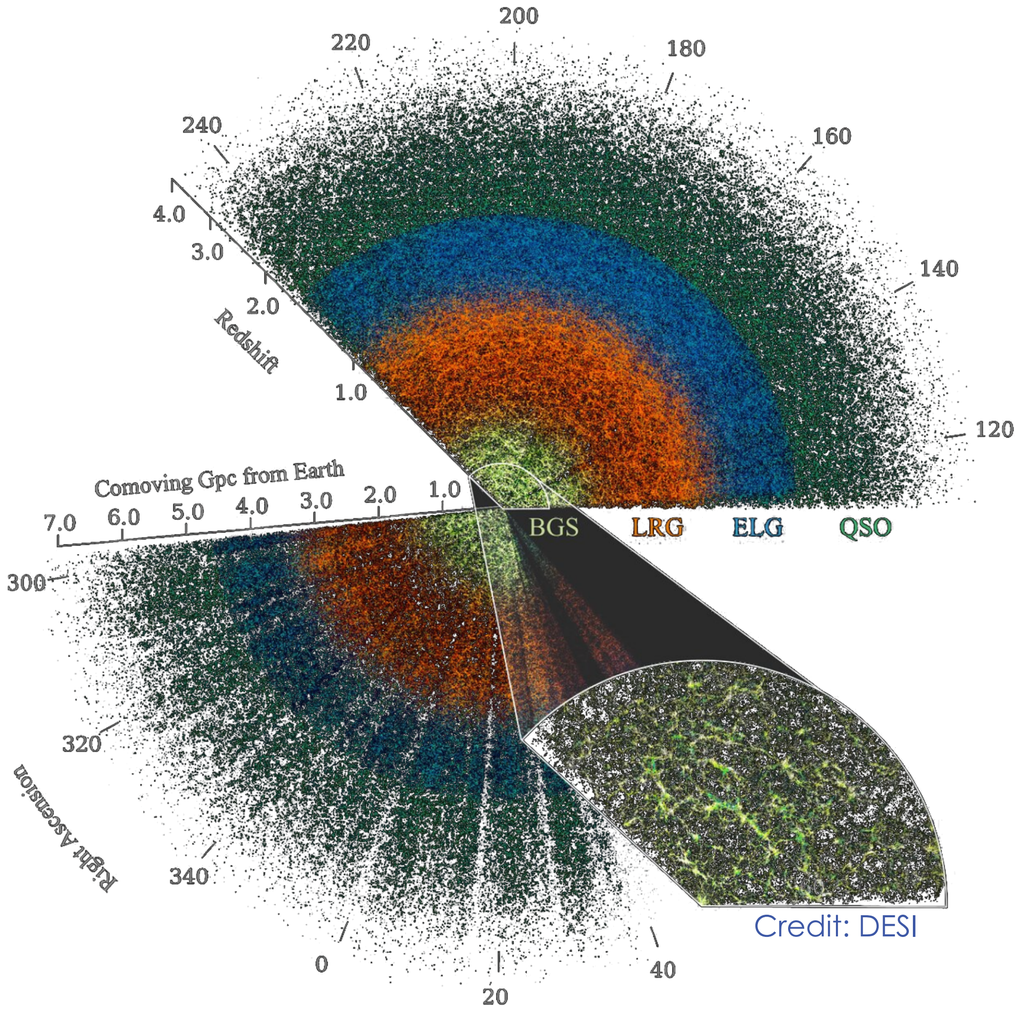


CMB temperature anisotropies



CMB lensing

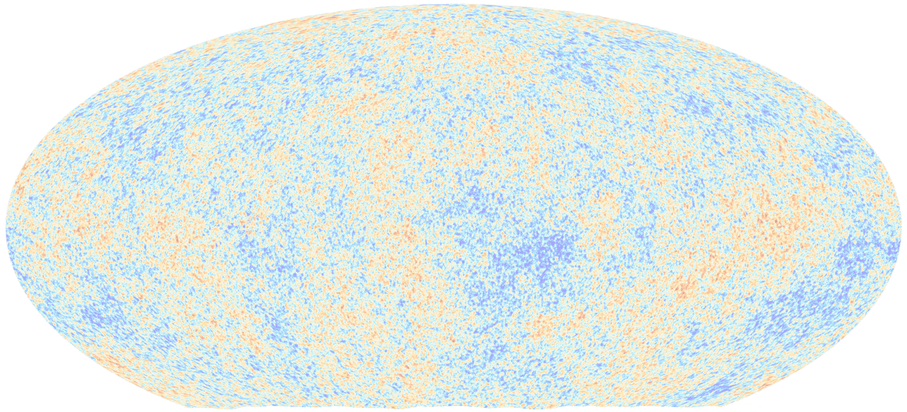
×

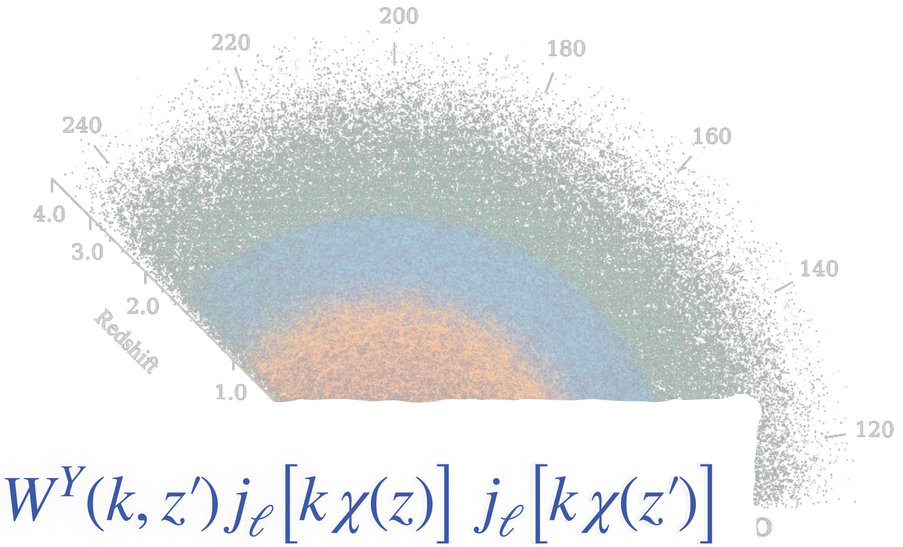


High z large-scale structure tracers

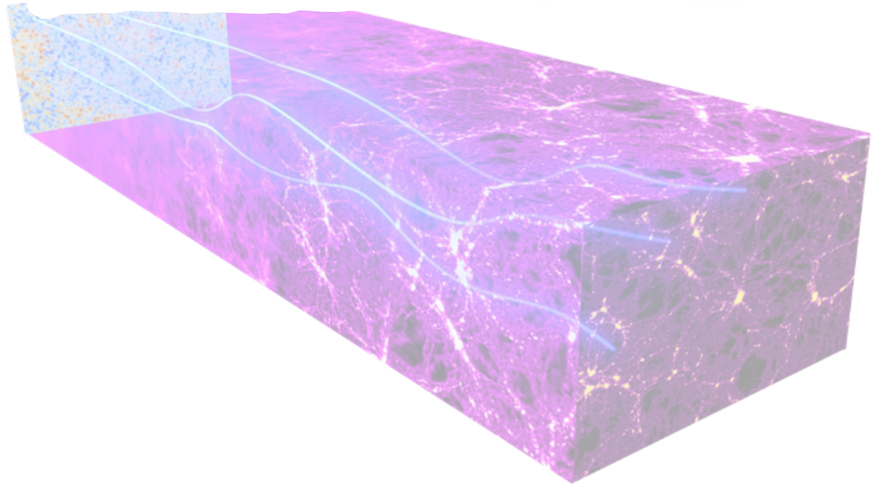
AGNs

Cross-correlations



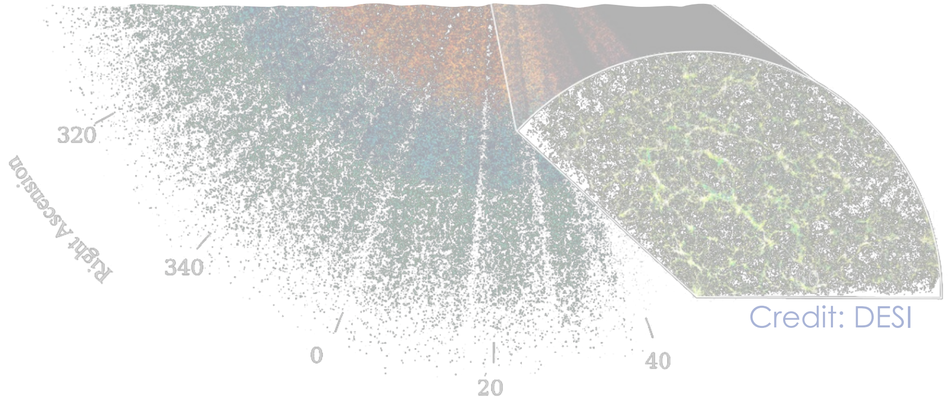


$$C_\ell^{\mathrm{X}\times\mathrm{Y}} = \frac{2}{\pi}\int_0^\infty dz \int_0^\infty dz' \int_0^\infty dk\, k^2 P_{\delta\delta}\left(k, z, z'\right) W^X(k, z)\, W^Y(k, z')\, j_\ell\left[k\chi(z)\right]\, j_\ell\left[k\chi(z')\right]$$



$$C_\ell^{\mathrm{T}\times\mathrm{GC}}$$

$$C_\ell^{\kappa\times\mathrm{GC}}$$



CMB lensing

High z large-scale structure tracers

AGNs

Why cross-correlations?

Less affected by systematics

$$b_g^{NG}(k,z) \propto \frac{f_{NL}}{k^2}$$

$f_{\rm NL}$ is strong at low ℓs, where systematics dominate

Break degeneracies!

$$C_\ell^{GC\times GC} \propto b^2\sigma_8^2, \quad C_\ell^{\kappa\times GC} \propto b\,\sigma_8^2$$

Test specific physical effects!

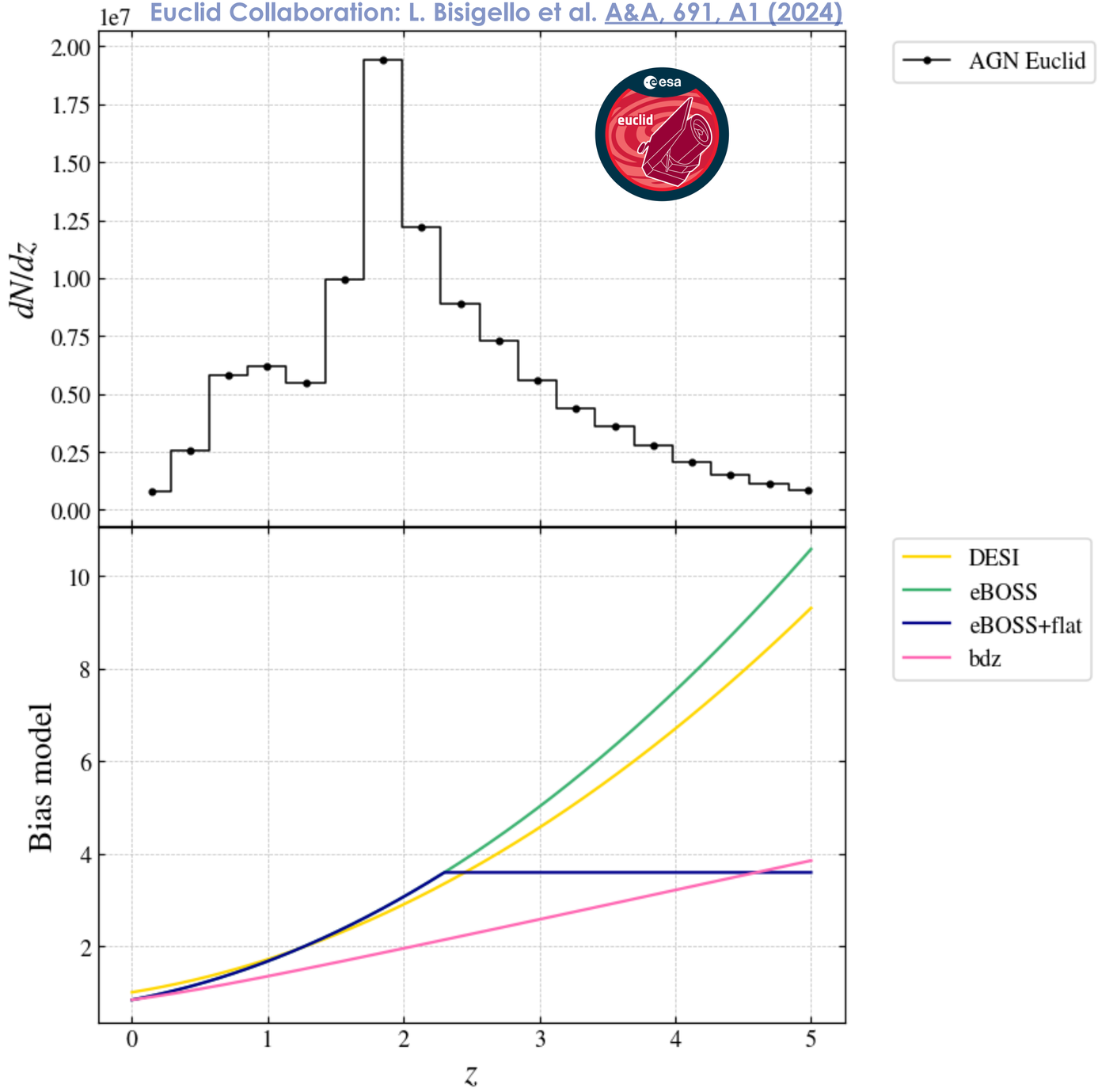
$$C_\ell^{T\times GC} \simeq C_\ell^{ISW\times GC}$$

Euclid AGNs sample (forecast)

$N_{\text{sources}} \sim 28 \cdot 10^6$

$f_{\text{sky}} = 36\,\%$

Euclid Collaboration: L. Bisigello et al. A&A, 691, A1 (2024)

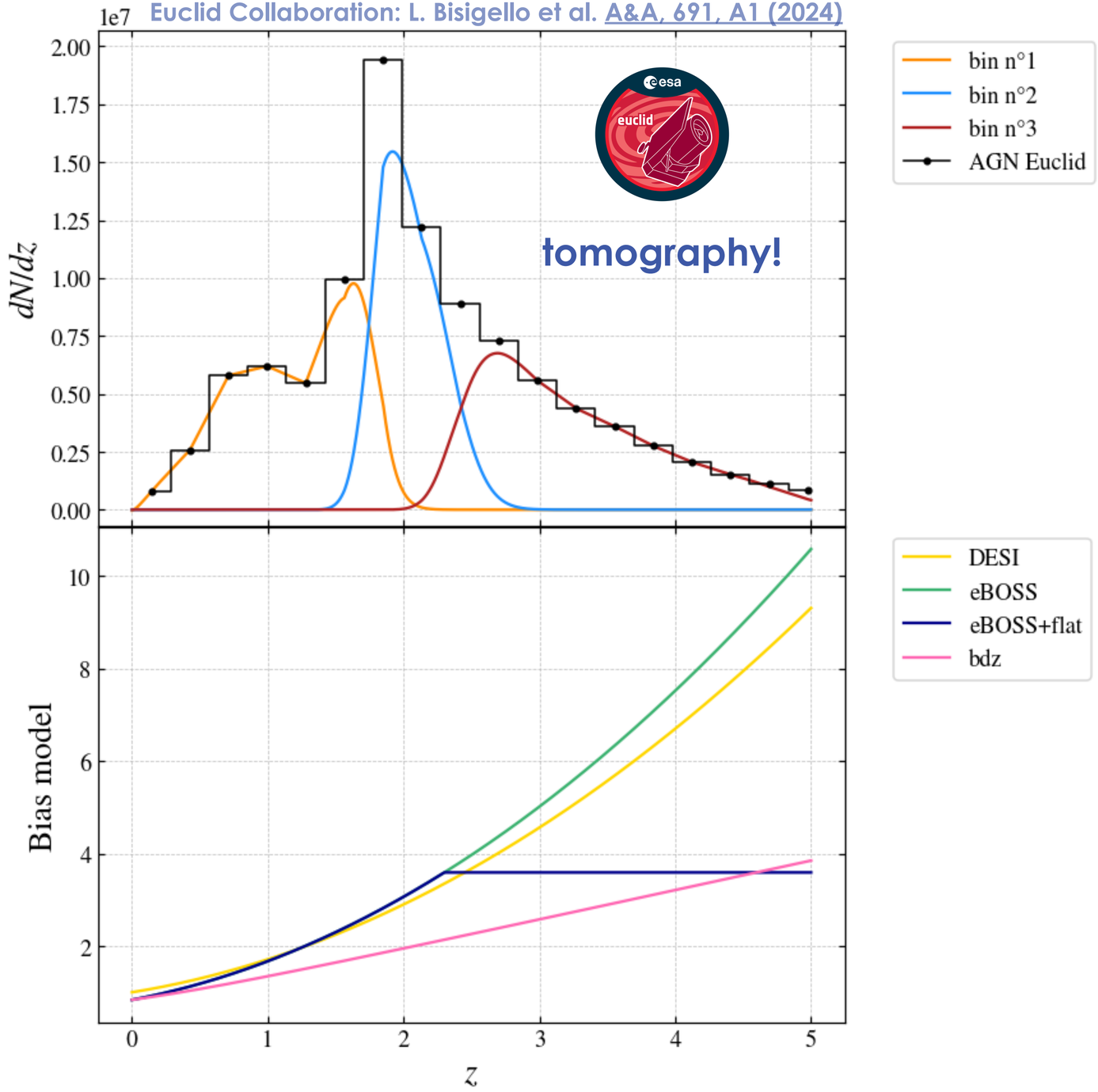


Euclid AGNs sample (forecast)

$N_{\text{sources}} \sim 28 \cdot 10^6$

$f_{\text{sky}} = 36\,\%$

Euclid Collaboration: L. Bisigello et al. A&A, 691, A1 (2024)



Euclid AGNs sample (forecast)

$N_{\text{sources}} \sim 28 \cdot 10^6$

$f_{\text{sky}} = 36\,\%$

$$\frac{dN}{dz} \longrightarrow$$

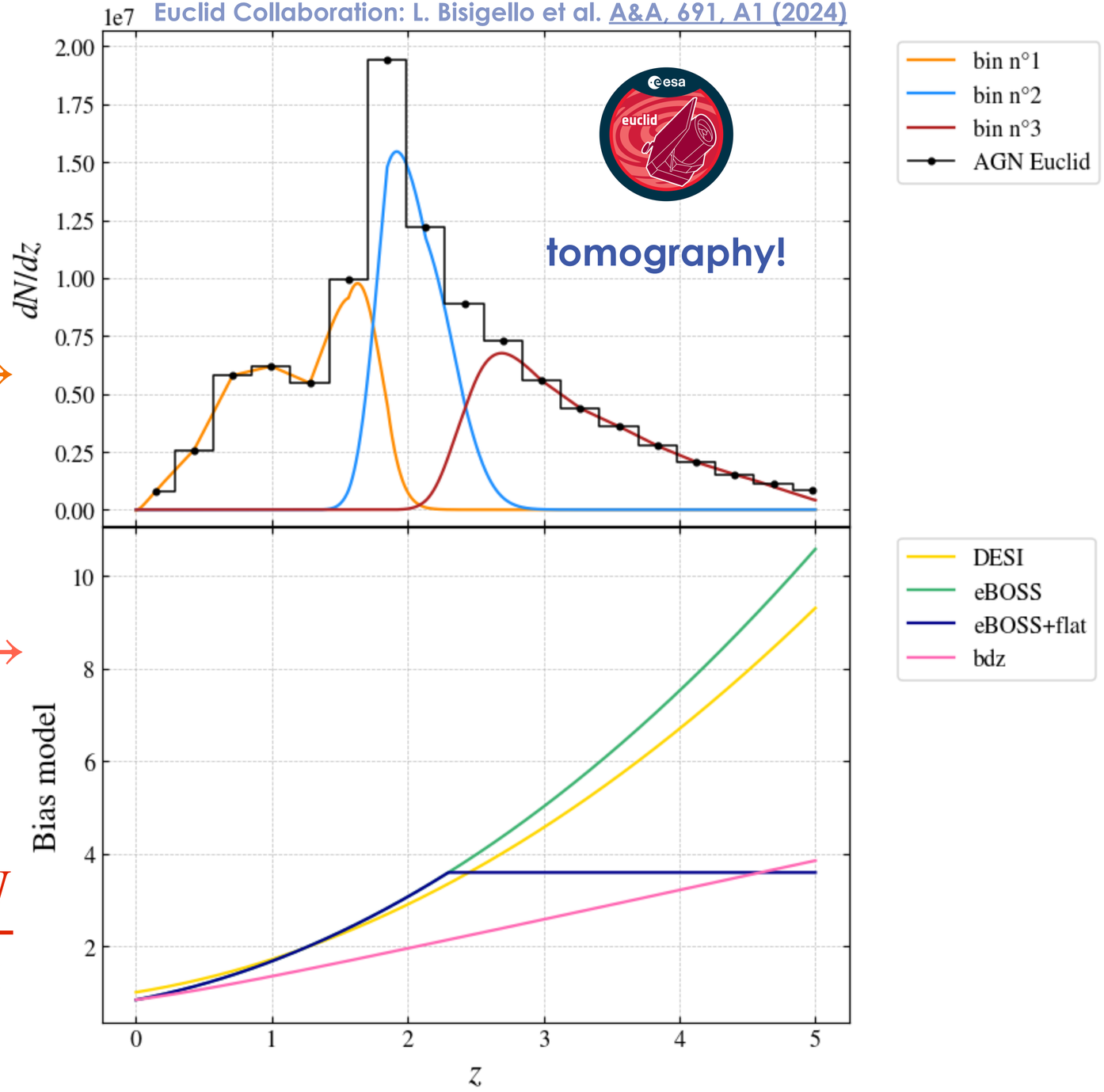
$$+$$

$$b_*(z) \longrightarrow$$

$$\Downarrow$$

$$W^{\text{GC}}(z) = b(z)\frac{dN}{dz}$$

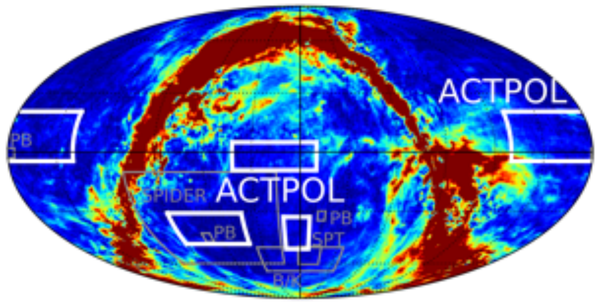
Euclid Collaboration: L. Bisigello et al. A&A, 691, A1 (2024)



CMB surveys

Planck

$$W^{\kappa}(z) = \frac{3}{2}\Omega_{m,0}\left(\frac{H_0}{c}\right)^2 \frac{c}{H(z)}(1+z)\chi(z)\left(\frac{\chi_* - \chi(z)}{\chi_*}\right)$$



Atacama Cosmology Telescope

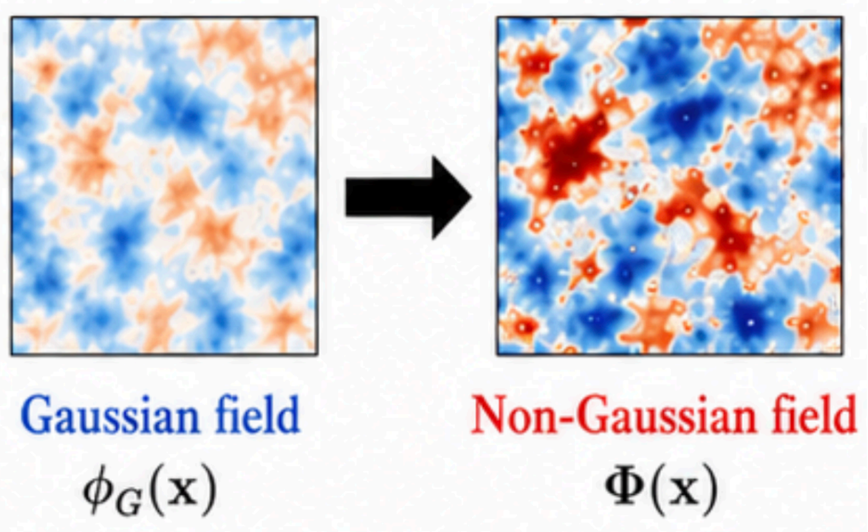
Simon's Observatory (forecast)

$$W^{\mathrm{ISW}}(k,z) = -\frac{3\Omega_{m,0}H_0^2}{c^3k^2}H(z)\frac{d}{dz}\left[D(z)(1+z)\right]$$

Primordial non-Gaussianity (PNG) f_{NL}

$$\Phi_{\mathrm{NG}}(x) = \phi_{\mathrm{G}}(x) + f_{\mathrm{NL}}\left(\phi_{\mathrm{G}}^2(x) - \left\langle \phi_{\mathrm{G}}^2 \right\rangle\right)$$

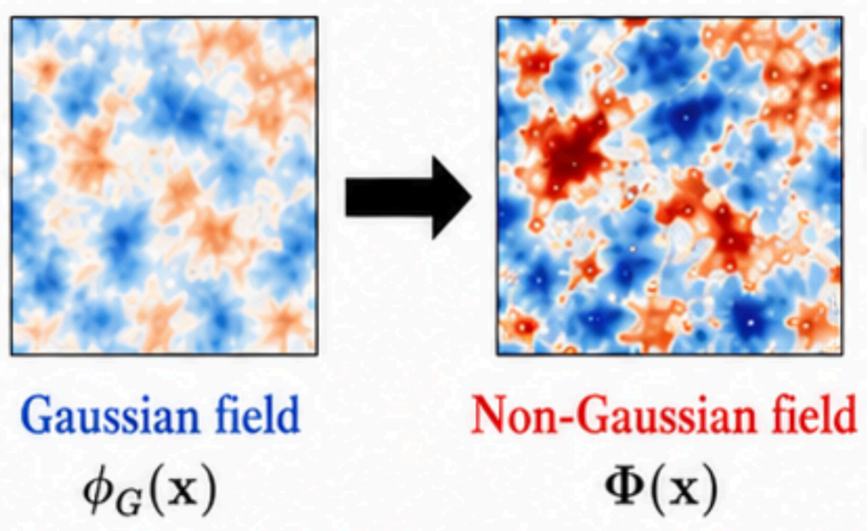
f_{NL} quantifies the departure from Gaussian initial conditions in the primordial potential field



Primordial non-Gaussianity (PNG) $f_{\rm NL}$

$$\Phi_{\rm NG}(x) = \phi_{\rm G}(x) + f_{\rm NL}\left(\phi_{\rm G}^2(x) - \left\langle \phi_{\rm G}^2 \right\rangle\right)$$

$f_{\rm NL}$ quantifies the departure from Gaussian initial conditions in the primordial potential field



$$b_g^{\rm NG}(k,z) = b_g(z)\left[1 + f_{\rm NL}\cdot 3\,\frac{b_g(z) - p_\phi}{b_g(z)}\,\frac{\Omega_{m,0}\,\delta_c}{k^2\,T(k)\,D(z)}\,\frac{H_0^2}{c^2}\right]$$

Local PNG induces a scale-dependent bias correction which is strongest on the larger scales

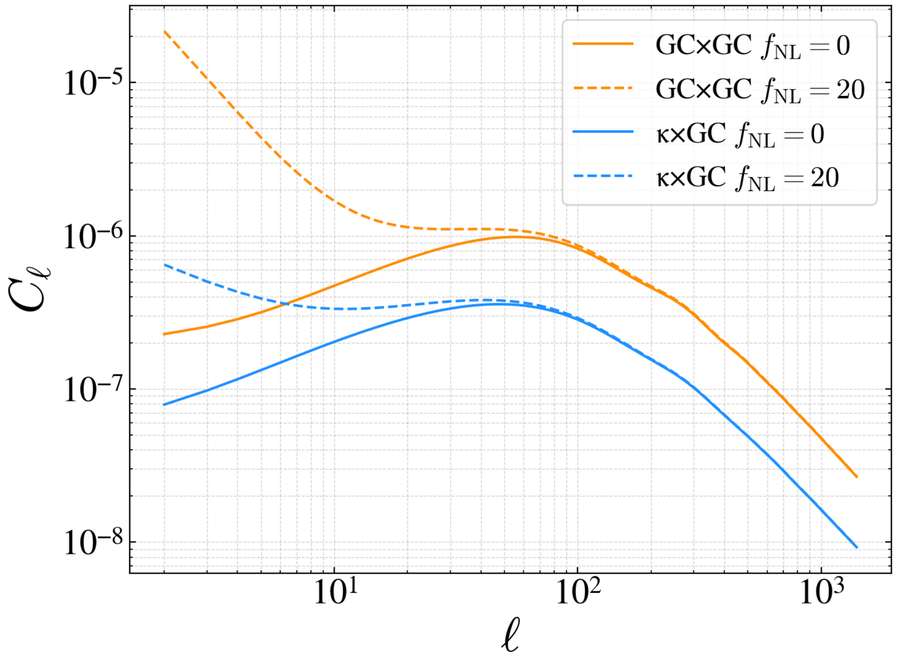
N. Dalal et al. 2008, Phys. Rev. D, 77, 123514
S. Matarrese and L. Verde 2008 ApJ 677 L77

$$\Delta b_{f_{\rm NL}} \propto \frac{f_{\rm NL}}{k^2}$$

Primordial non-Gaussianity (PNG) $f_{\rm NL}$

$$\Phi_{\rm NG}(x) = \phi_{\rm G}(x) + f_{\rm NL}\left(\phi_{\rm G}^2(x) - \left\langle \phi_{\rm G}^2 \right\rangle\right)$$

$f_{\rm NL}$ quantifies the departure from Gaussian initial conditions in the primordial potential field



$$b_g^{\rm NG}(k,z) = b_g(z)\left[1 + f_{\rm NL}\cdot 3\,\frac{b_g(z) - p_\phi}{b_g(z)}\,\frac{\Omega_{m,0}\,\delta_c}{k^2\,T(k)\,D(z)}\,\frac{H_0^2}{c^2}\right]$$

Local PNG induces a scale-dependent bias correction which is strongest on the larger scales

N. Dalal et al. 2008, Phys. Rev. D, 77, 123514
S. Matarrese and L. Verde 2008 ApJ 677 L77

$$\Delta b_{f_{\rm NL}} \propto \frac{f_{\rm NL}}{k^2}$$

Amplitude of matter perturbations $\sigma_8(z)$

$$\sigma_8^2(z) = \int_0^\infty dk \frac{k^2 P_{\rm lin}(k,z)}{2\pi^2} \left| W_8(k) \right|^2$$

We model the evolution of matter perturbations at different redshift ranges

Amplitude of matter perturbations $\sigma_8(z)$

$$\sigma_8^2(z) = \int_0^\infty dk \frac{k^2 P_{\rm lin}(k,z)}{2\pi^2} \left| W_8(k) \right|^2$$

We model the evolution of matter perturbations at different redshift ranges

We introduce a redshift-dependent parametrisation of the linear matter power spectrum

C. Embil-Villagra et al. JCAP12(2025)033

$$P_{\rm lin}^{\rm new}(k,z) = A(z)\, P_{\rm lin}(k,z)$$

Amplitude of matter perturbations $\sigma_8(z)$

$$\sigma_8^2(z) = \int_0^\infty dk \frac{k^2 P_{\rm lin}(k,z)}{2\pi^2} \left| W_8(k) \right|^2$$

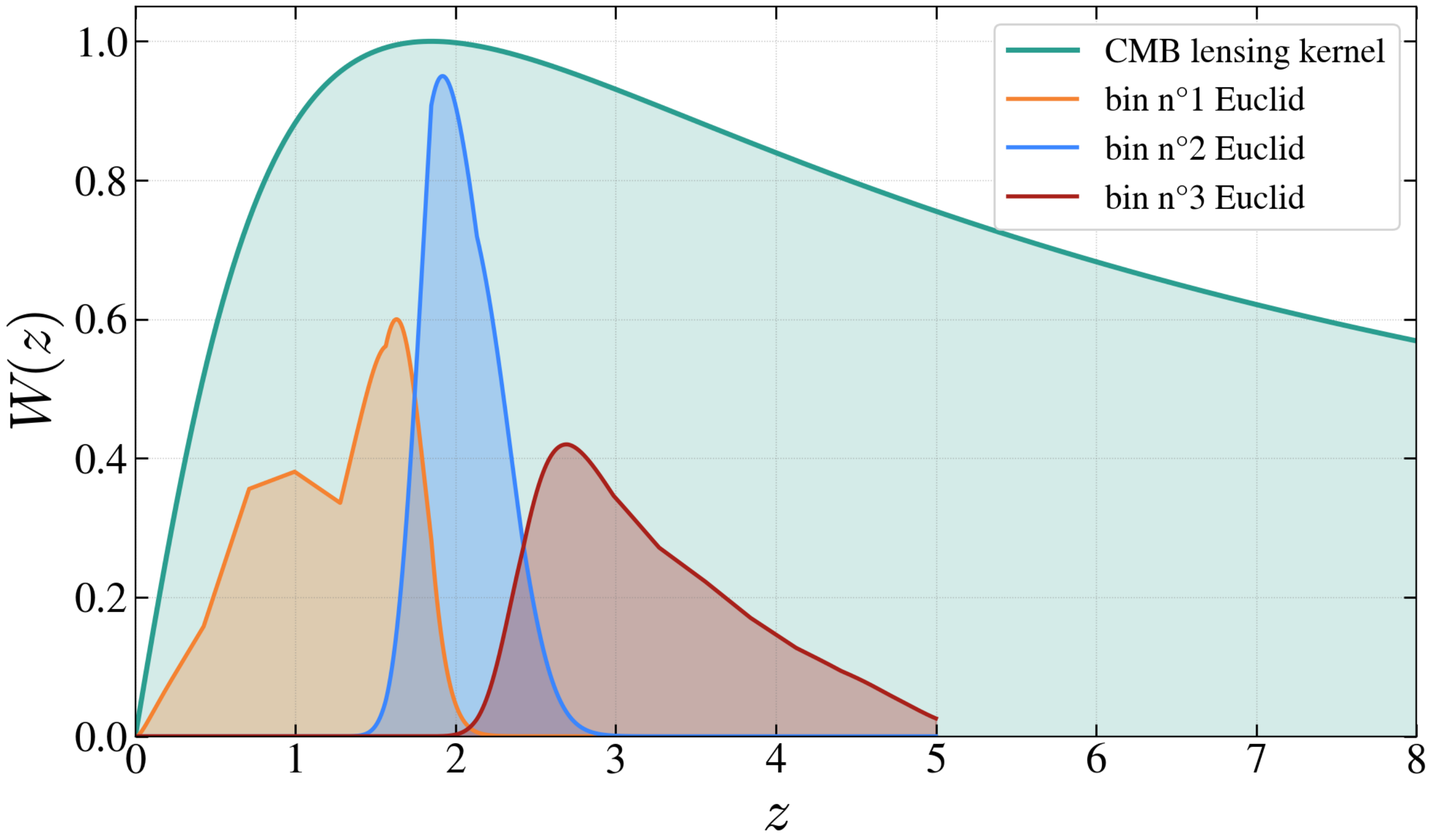
We model the evolution of matter perturbations at different redshift ranges

We introduce a redshift-dependent parametrisation of the linear matter power spectrum

C. Embil-Villagra et al. JCAP12(2025)033

$$P_{\rm lin}^{\rm new}(k,z) = A(z)\, P_{\rm lin}(k,z)$$

$$A(z) = \begin{cases} A_1 & 0 \le z < z_1 \ (\kappa\times\text{GC}) \\ A_2 & z_1 \le z < z_2 \ (\kappa\times\text{GC}) \\ A_3 & z_2 \le z < z_3 \ (\kappa\times\text{GC}) \\ A_4 & z_3 \le z \qquad (\kappa\times\kappa) \end{cases}$$

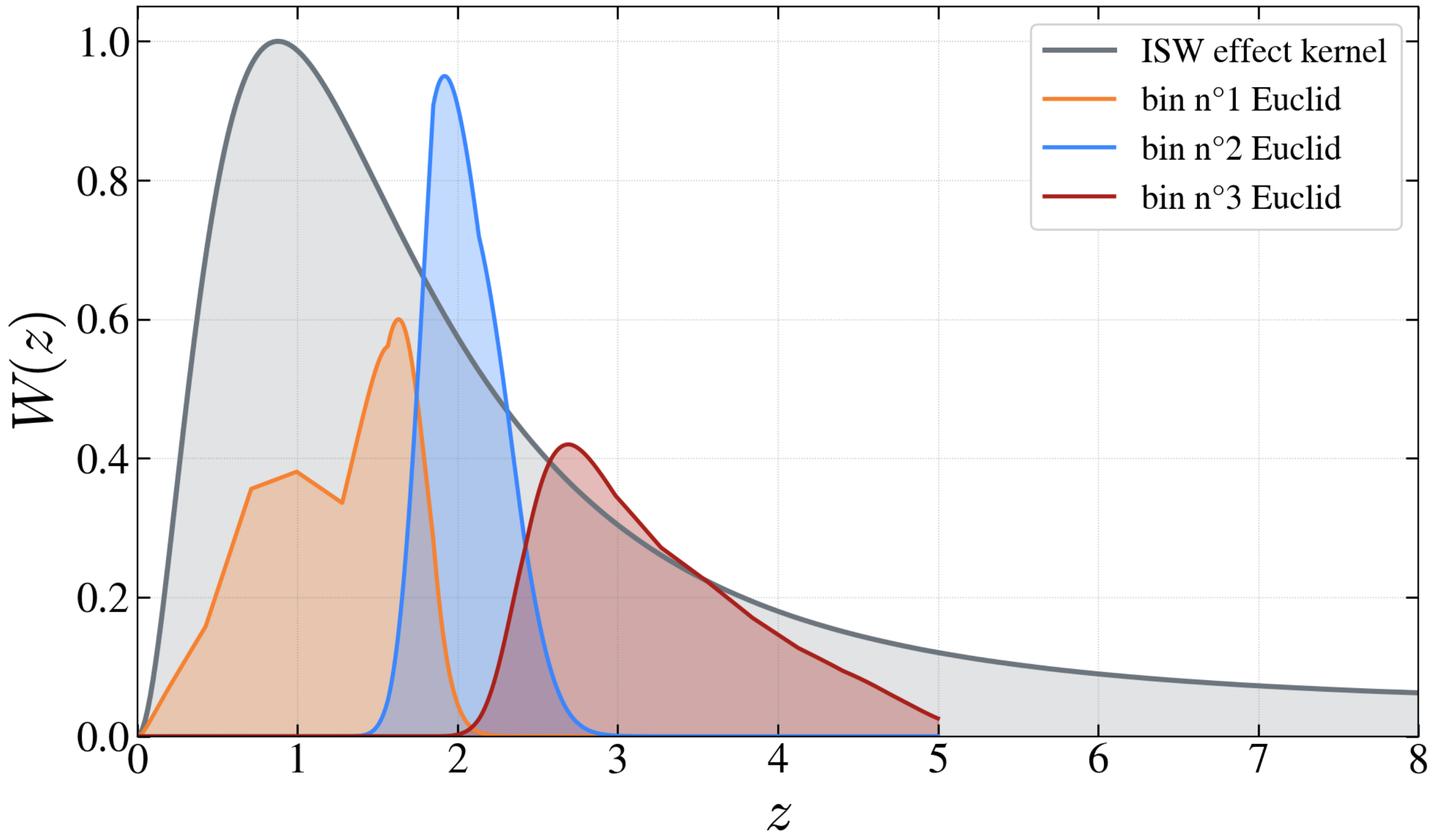


Dark energy e.o.s w_0 and density parameter Ω_Λ^0

For late-time ISW, the kernel peaks at lower redshifts than AGN's kernel

$\Longrightarrow$

Consequently we have a low S/N, and expect non-tight constraints



Dark energy e.o.s w_0 and density parameter Ω_Λ^0

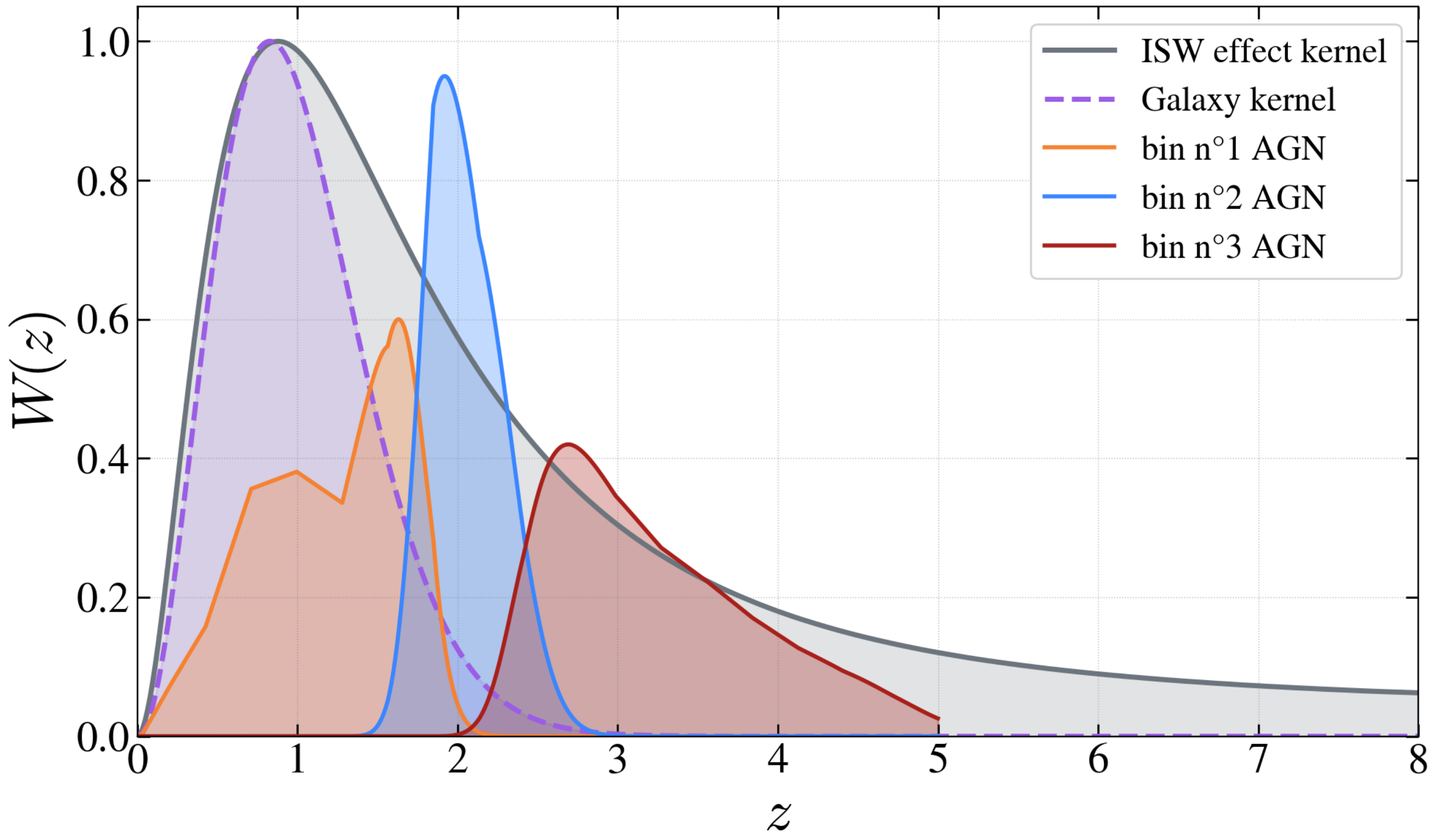
For late-time ISW, the kernel peaks at lower redshifts than AGN's kernel

$\Longrightarrow$

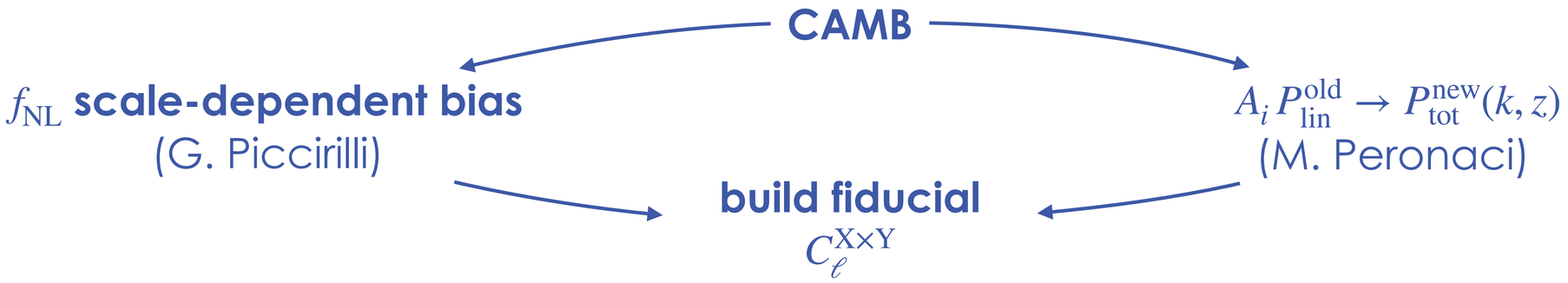
Consequently we have a low S/N, and expect non-tight constraints

BUT

It still is a complementary measurement to galaxies at high redshifts



Methodology



Methodology

CAMB

$f_{\rm NL}$ **scale-dependent bias**
(G. Piccirilli)

$A_i\, P_{\rm lin}^{\rm old} \to P_{\rm tot}^{\rm new}(k,z)$
(M. Peronaci)

build fiducial
$C_\ell^{\rm X\times Y}$

$$\mathrm{Cov}\left(C_\ell^{AB}, C_{\ell'}^{CD}\right) = \frac{1}{(2\ell+1) f_{\rm sky}^{AB} f_{\rm sky}^{CD}} \times$$

$$\times \left[f_{\rm sky}^{AC,BD} \sqrt{C_\ell^{AC} C_{\ell'}^{AC} C_\ell^{BD} C_{\ell'}^{BD}} + f_{\rm sky}^{AD,BC} \sqrt{C_\ell^{AD} C_{\ell'}^{AD} C_\ell^{BC} C_{\ell'}^{BC}} \right] \delta_{\ell\ell'}$$

model the covariance, run a MCMC

	$f_{\rm NL}$	b_i	A_i	w_0	Ω_Λ^0
priors	$\mathcal{U}(-50,50)$	$\mathcal{U}(0,2)$	$\mathcal{U}(0,2)$	$\mathcal{U}(-2,-1/3)$	$\mathcal{U}(0,0.948)$

Methodology

CAMB

$f_{\rm NL}$ **scale-dependent bias**
(G. Piccirilli)

$A_i\, P_{\rm lin}^{\rm old} \rightarrow P_{\rm tot}^{\rm new}(k,z)$
(M. Peronaci)

build fiducial
$C_\ell^{\rm X\times Y}$

$$\mathrm{Cov}\left(C_\ell^{AB}, C_{\ell'}^{CD}\right) = \frac{1}{(2\ell+1) f_{\rm sky}^{AB} f_{\rm sky}^{CD}} \times$$

$$\times \left[f_{\rm sky}^{AC,BD} \sqrt{C_\ell^{AC} C_{\ell'}^{AC} C_\ell^{BD} C_{\ell'}^{BD}} + f_{\rm sky}^{AD,BC} \sqrt{C_\ell^{AD} C_{\ell'}^{AD} C_\ell^{BC} C_{\ell'}^{BC}} \right] \delta_{\ell\ell'}$$

model the covariance, run a MCMC

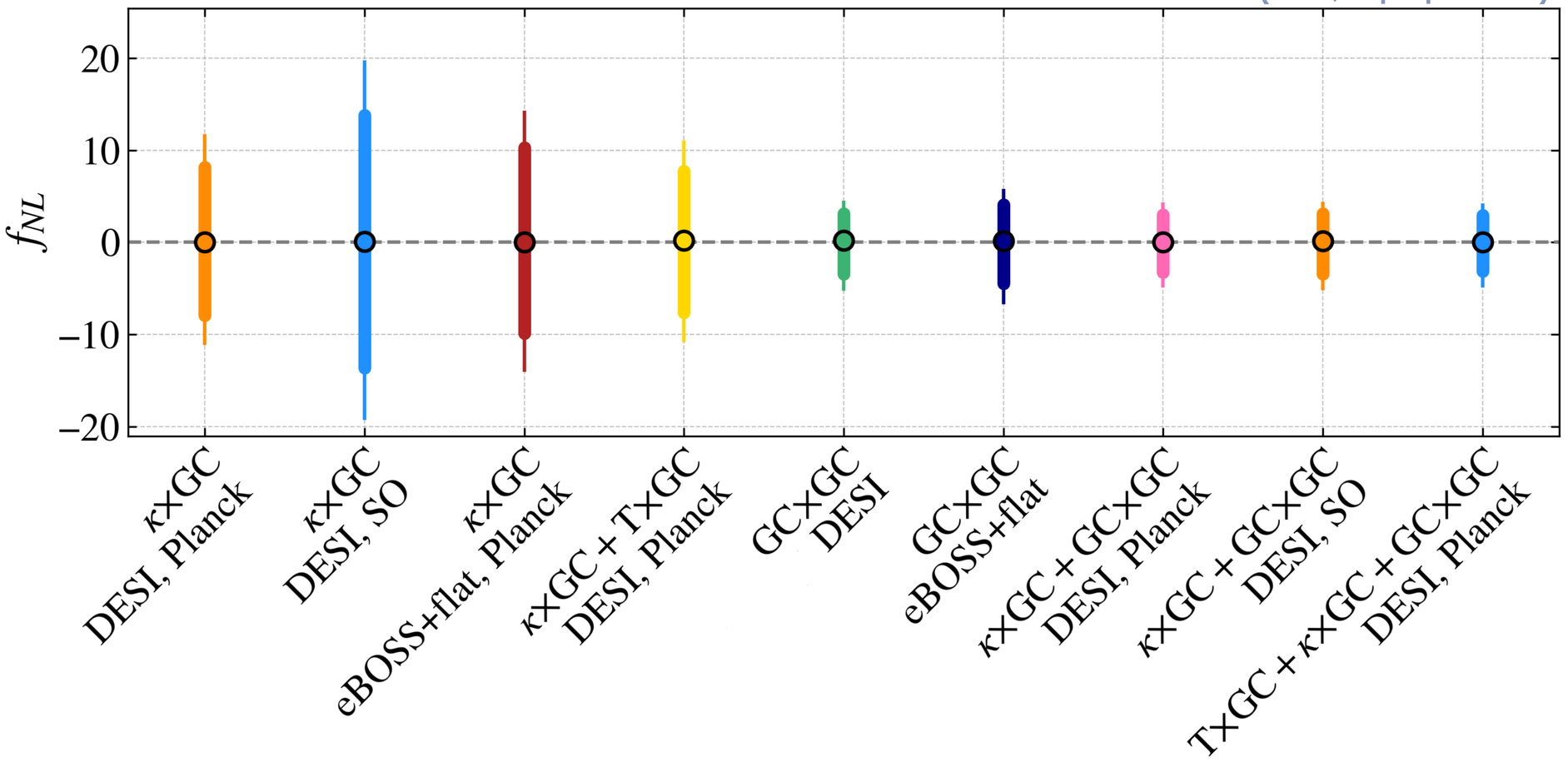
	$f_{\rm NL}$	b_i	A_i	w_0	Ω_Λ^0
priors	$\mathcal{U}(-50,50)$	$\mathcal{U}(0,2)$	$\mathcal{U}(0,2)$	$\mathcal{U}(-2,-1/3)$	$\mathcal{U}(0,0.948)$

since these are forecasts, we are only interested in the constraining power of the quantities:

$$\sigma_{f_{\rm NL}},\ \sigma_{b_i},\ \sigma_{A_i},\ \sigma_{w_0},\ \sigma_{\Omega_\Lambda^0}$$

Results – Primordial non-Gaussianity $f_{\rm NL}$

M. Peronaci et al. (2026, in preparation)

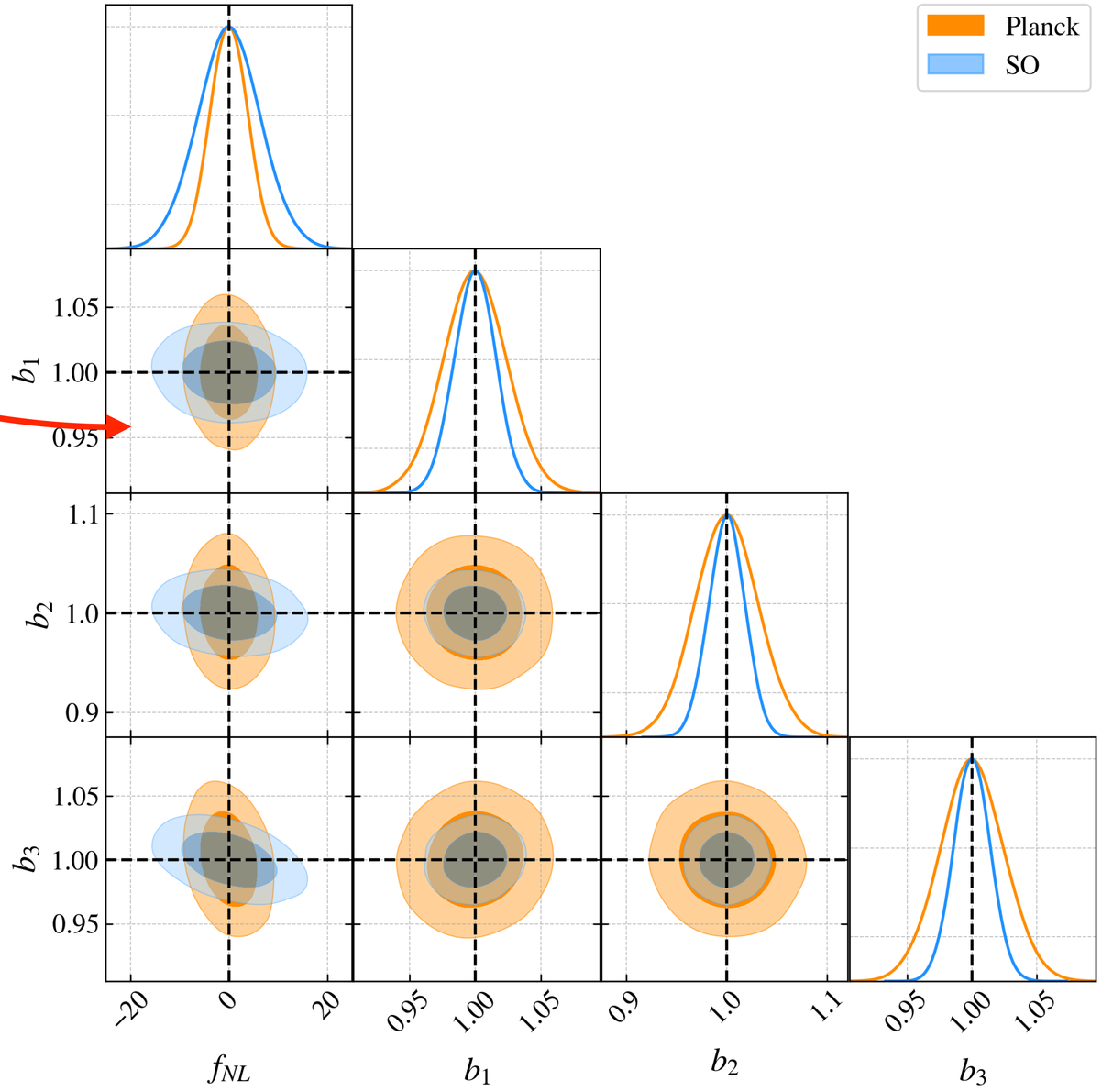


with Euclid DR3 we expect $\sigma_{f_{\rm NL},\,\rm best} \approx 2.5$ **vs** $\sigma_{f_{\rm NL}} \approx 17$ **from comparable analyses**

N.B. "DESI", "eBOSS+flat" are the AGN bias models assumed
N.B. "Planck", "SO" are the lensing noise curves

Results – Primordial non-Gaussianity $f_{\rm NL}$

When considering just the cross-correlation $\kappa \times$ GC with Planck and SO, there is a "rotation" in the correlation due to the CMB κ survey



M. Peronaci et al. (2026, in preparation)

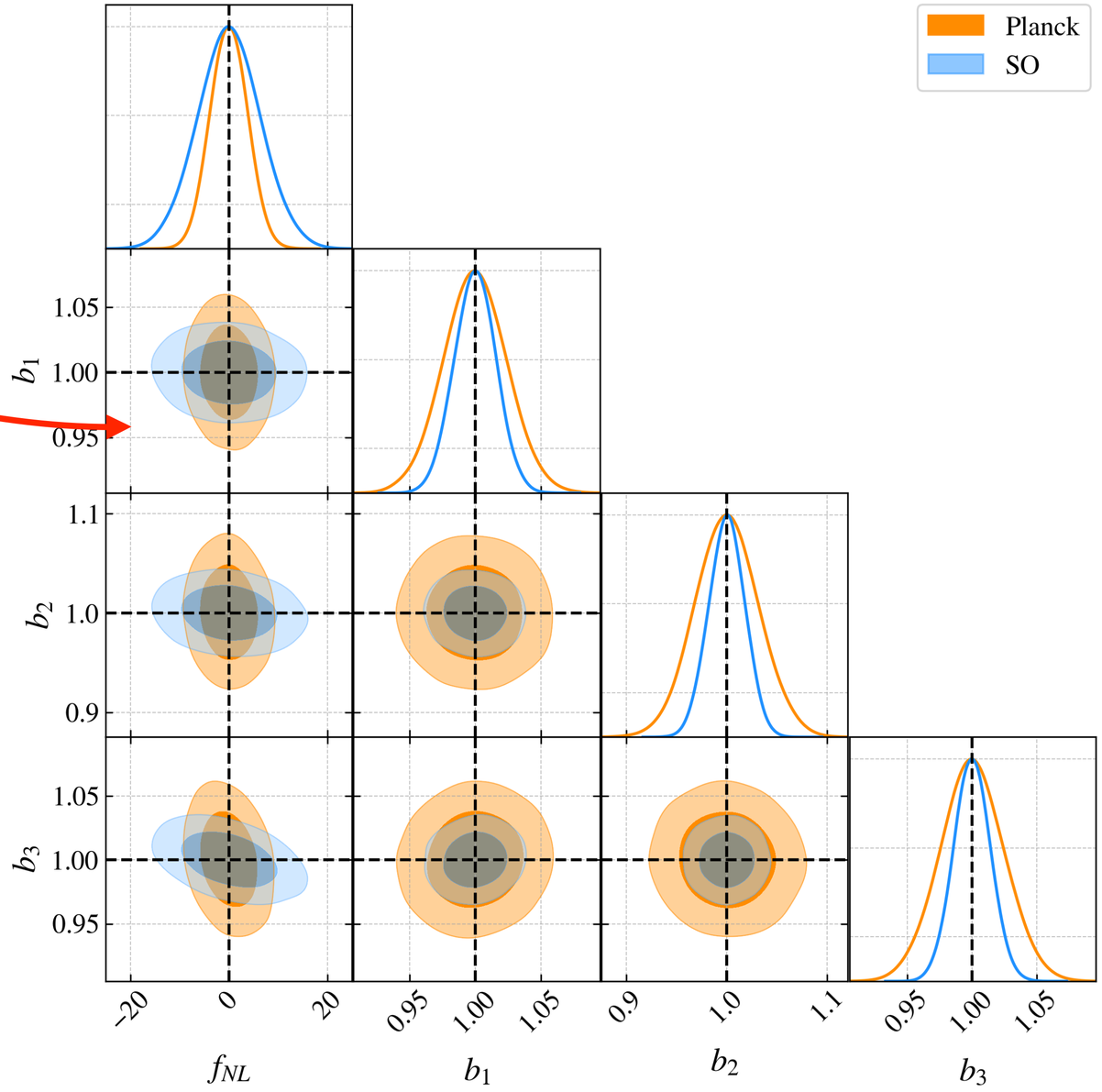
Results – Primordial non-Gaussianity $f_{\rm NL}$

When considering just the cross-correlation $\kappa \times$ GC with Planck and SO, there is a "rotation" in the correlation due to the CMB κ survey

Planck has higher lensing noise
$\Longrightarrow$ less constraining power on the bias

SO has limited multipole ranges
$\Longrightarrow$ less constraining power on the $f_{\rm NL}$

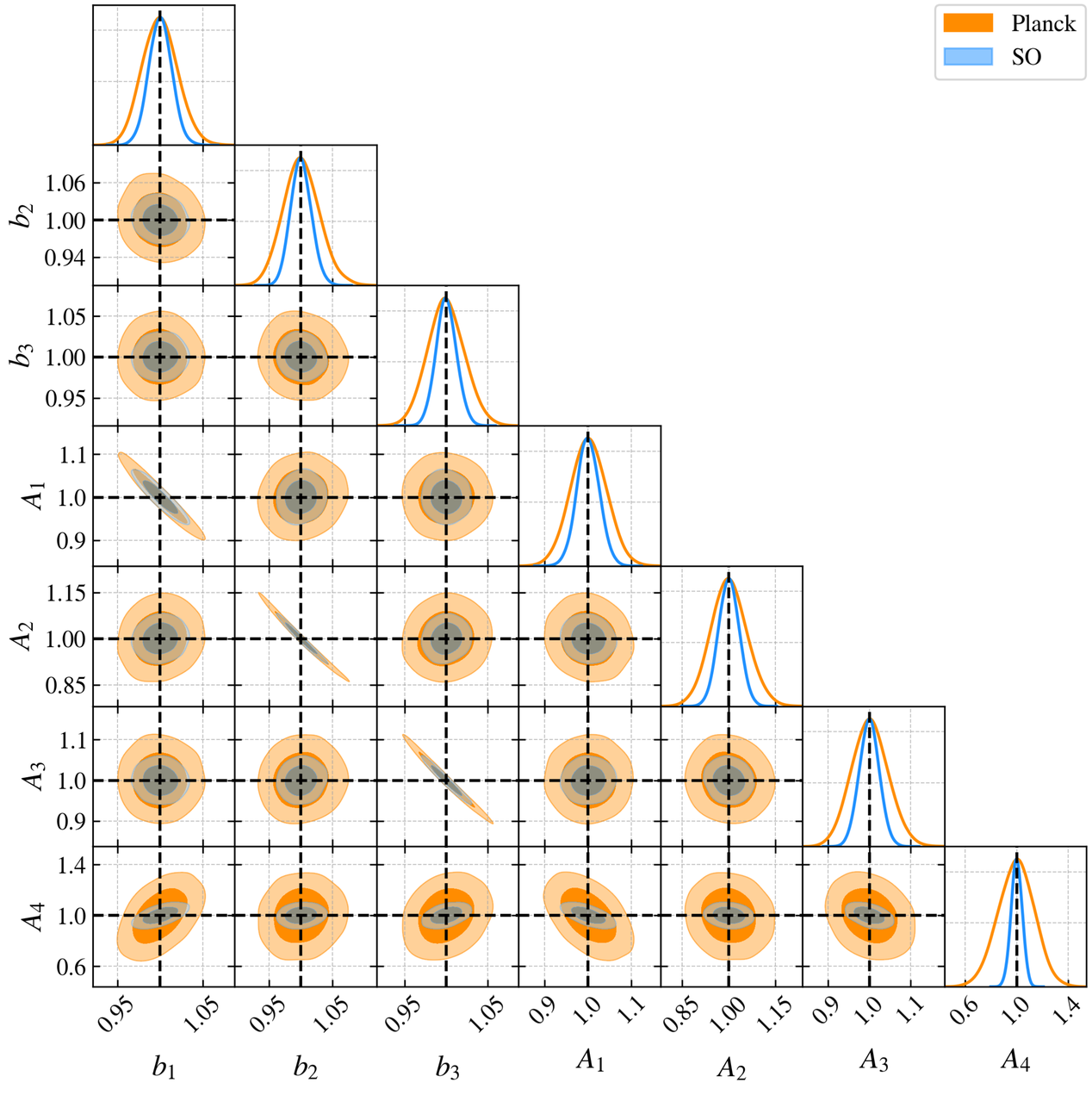
$$\ell^{\rm Planck}_{\kappa\times{\rm GC}} \in [4, 400], \ \ell^{\rm SO}_{\kappa\times{\rm GC}} \in [30, 3000]$$



M. Peronaci et al. (2026, in preparation)

Results – Amplitude of matter perturbations $\sigma_8(z)$

The combination of $\kappa\times\kappa + \kappa\times$GC+GC$\times$GC helps us fixing A_i for each redshift interval



M. Peronaci et al. (2026, in preparation)

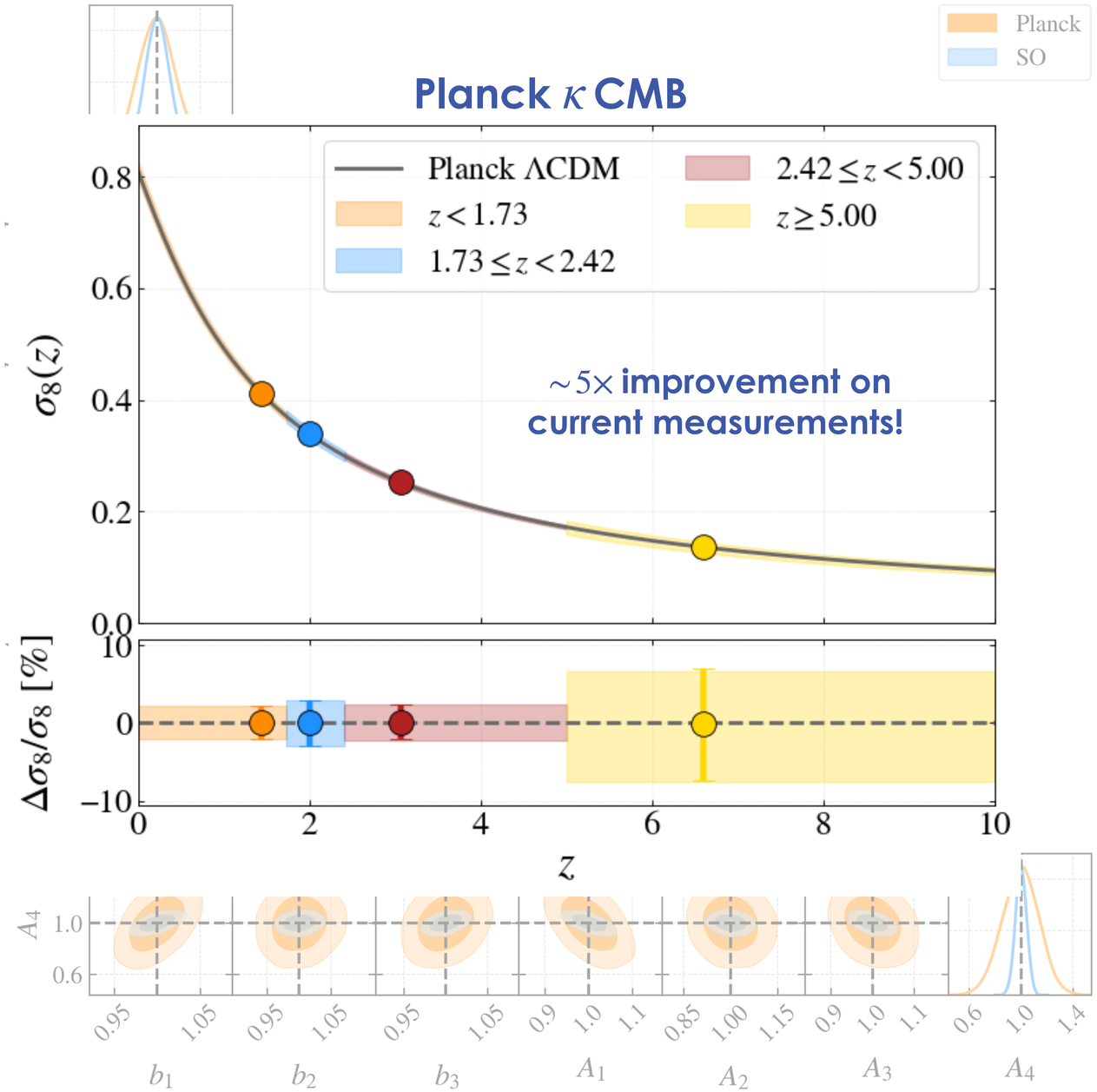
Results – Amplitude of matter perturbations $\sigma_8(z)$

The combination of $\kappa\times\kappa + \kappa\times$GC+GC$\times$GC helps us fixing A_i for each redshift interval

Once we have A_i we obtain unique measurements of structure growth at high redshifts

$$\tilde{\sigma}_8(z_i) = \sigma_8(z_i)\sqrt{A_i}$$

M. Peronaci et al. (2026, in preparation)

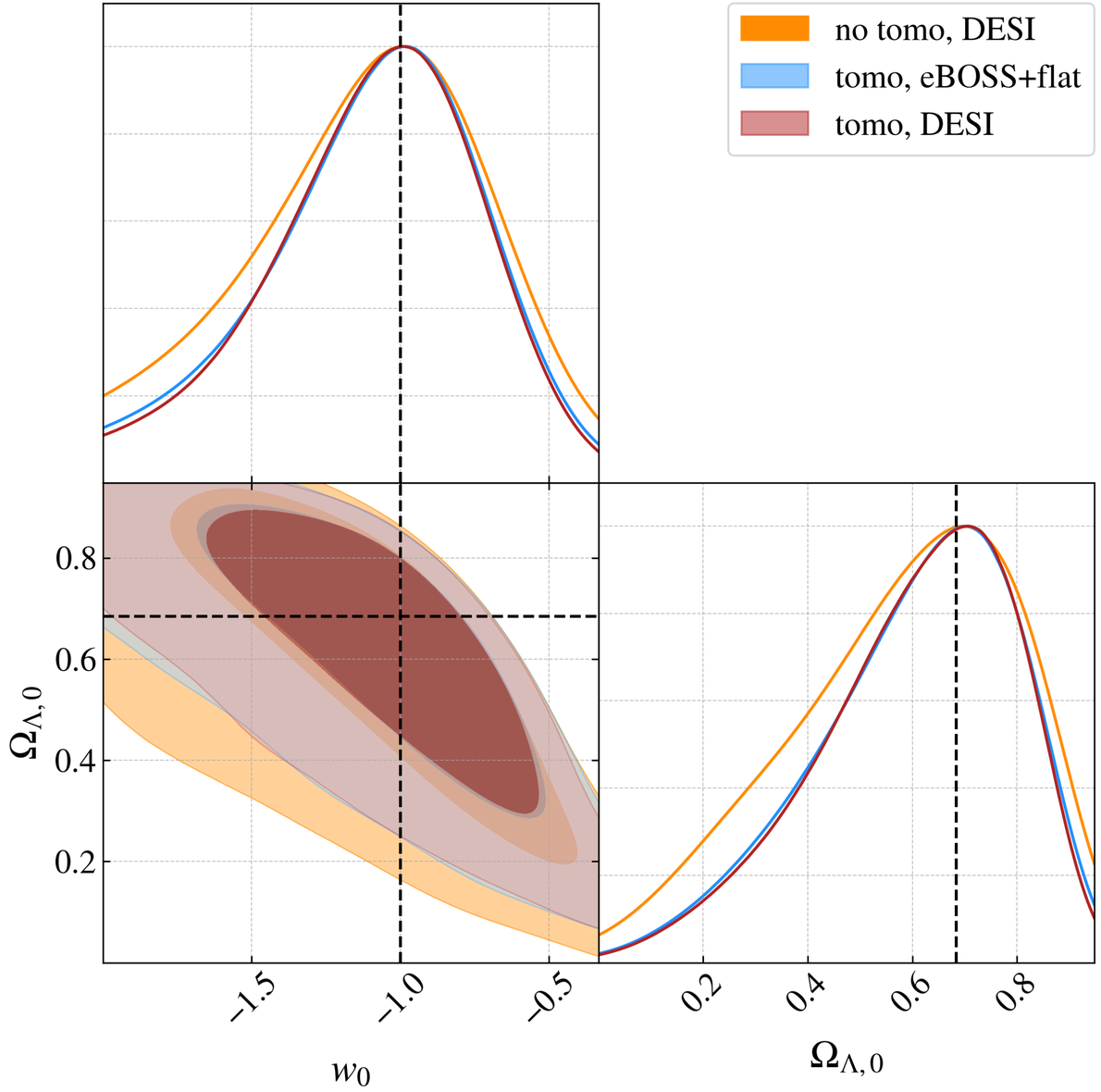


Results – Dark energy and density parameter w_0 , Ω_Λ^0

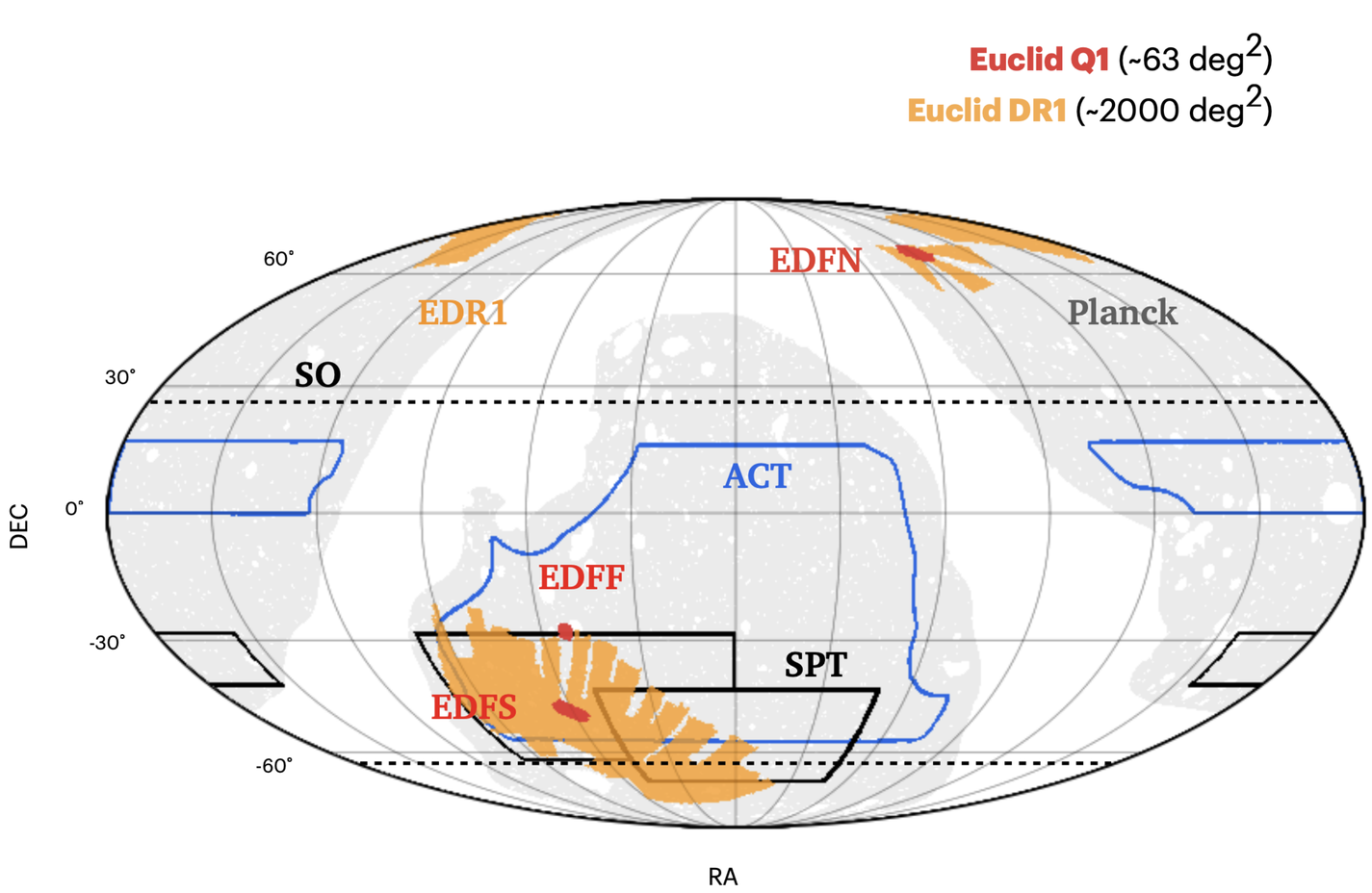
Assuming a ΛCDM model,
ISW with AGN is less constraining than with galaxies because $W^{\rm ISW}$ better overlaps with galaxy clustering…

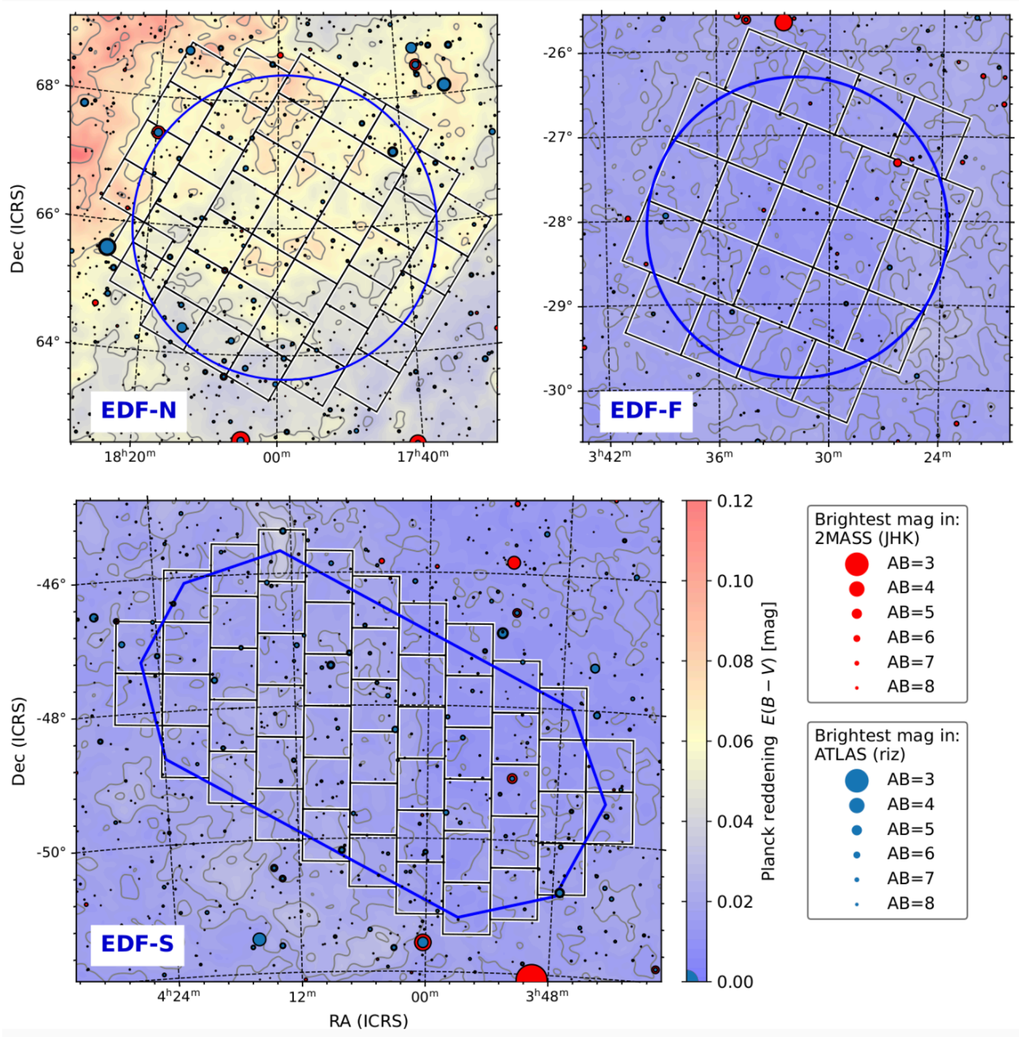
…But it still works as a high redshift complementary probe for ISW science!

M. Peronaci et al. (2026, in preparation)



From forecasts to Euclid data (Q1)





Data filtering and extraction of $N(z)$

Select required flags:

- [x] good_flags
- [ ] bright_vis_mag_bin
- [ ] medium_vis_mag_bin
- [ ] faint_vis_mag_bin
- [ ] PRF_qso_candidate
- [x] JH_IeY_qso_candidate
- [ ] IeH_gz_qso_candidate
- [ ] B24a_qso_candidate
- [ ] B24b_qso_candidate
- [ ] C75_agn_candidate
- [ ] R90_agn_candidate
- [ ] GDR3_qso_candidate

PDF Source:

- ( ) Most Probable (QSOV vs EXTNV)
- (•) Use QSOV Only
- ( ) Use EXTNV Only

- [ ] Require source to have a Spec-z

z-assignment:

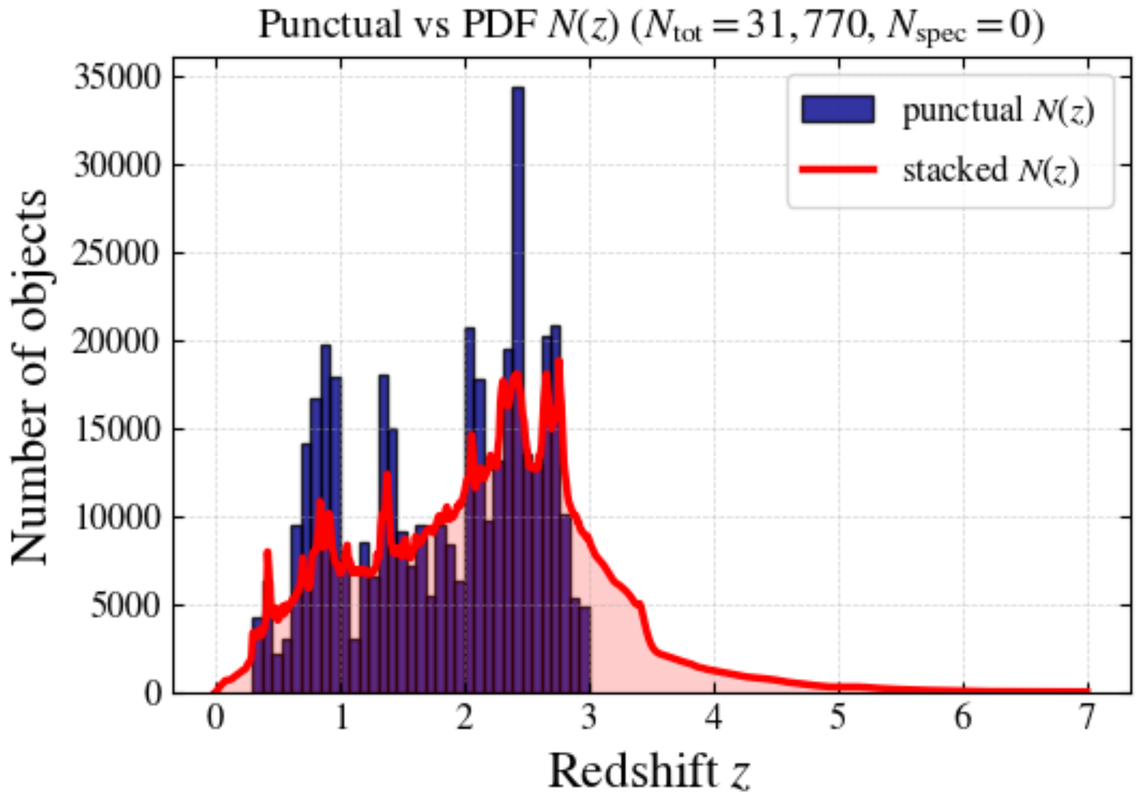
- ( ) Use spec-z when available
- (•) Photo-z only

Thresholds:

mumax (<):		−2.60
prob_GAL (<=):		1.00
prob_QSO (>=):		0.00
z_min (>=):		0.30
z_max (<=):		3.00

Photo-z estimation:
Euclid Collaboration: B. Laloux et al. A&A. (2026, accepted)

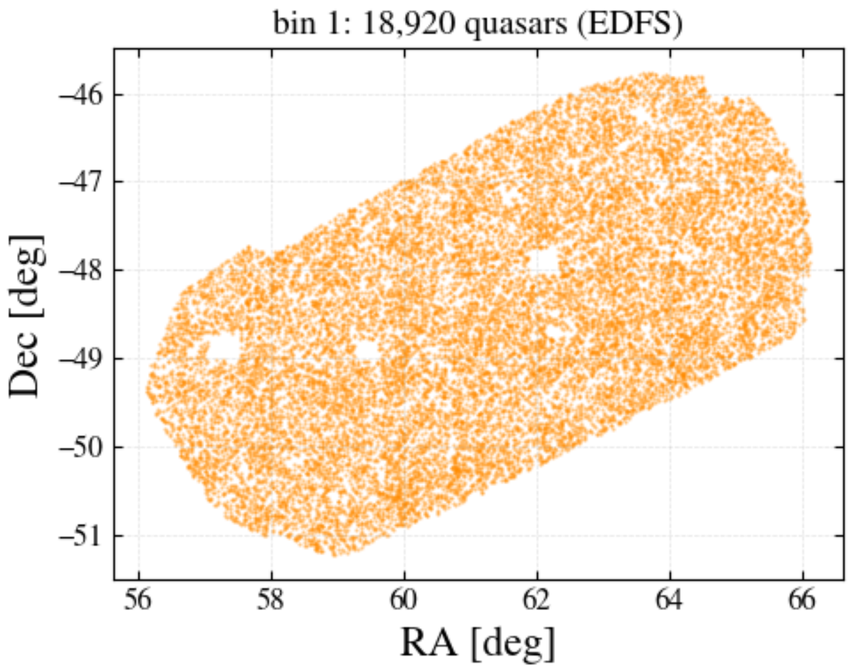
Multiwavelength data and AGN candidate color selection:
Euclid Collaboration: T. Matamoro-Zatarain et al. A&A, 711, A1 (2026)



Map making – AGNs

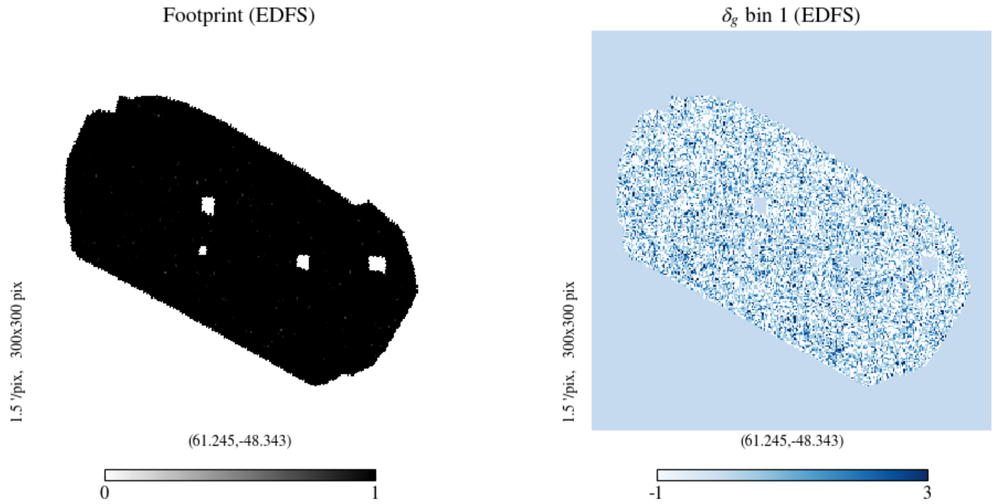
We use the filtered catalog to build an AGN overdensity map

Import extracted RA/Dec



$\Longrightarrow$

Build the overdensity map δ_g



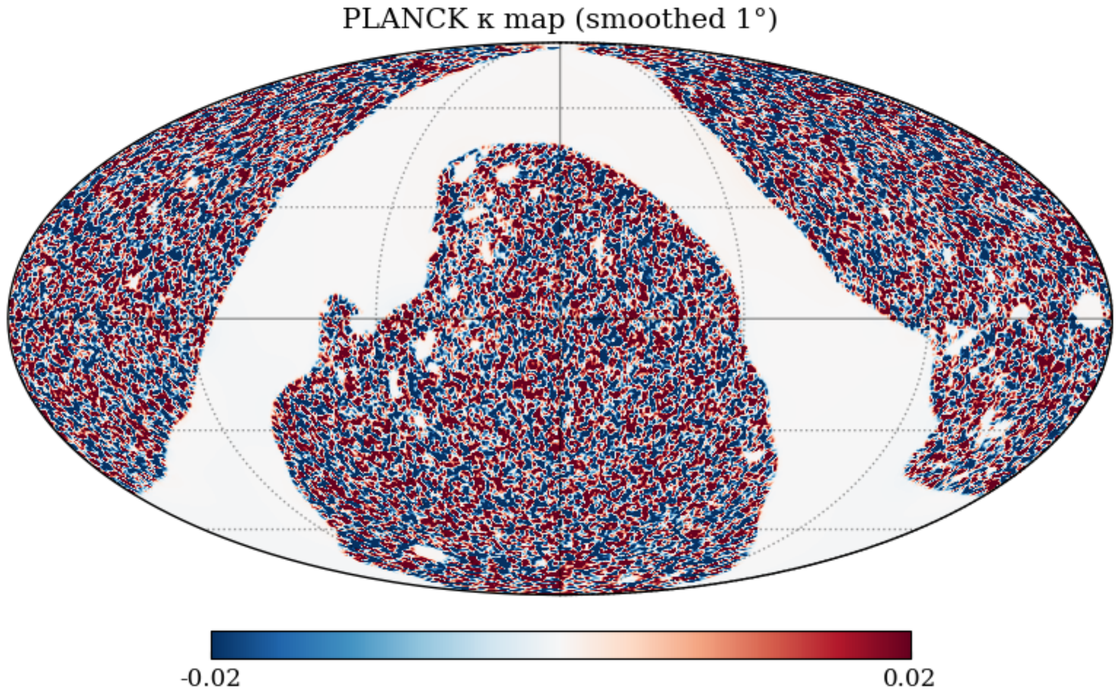
n_i: number of AGNs in pixel i

$$\bar{n} = \frac{\sum_{i \in \text{footprint}} n_i}{N_{\text{footprint}}} \Longrightarrow \delta_{g,i} = \frac{n_i}{\bar{n}} - 1$$

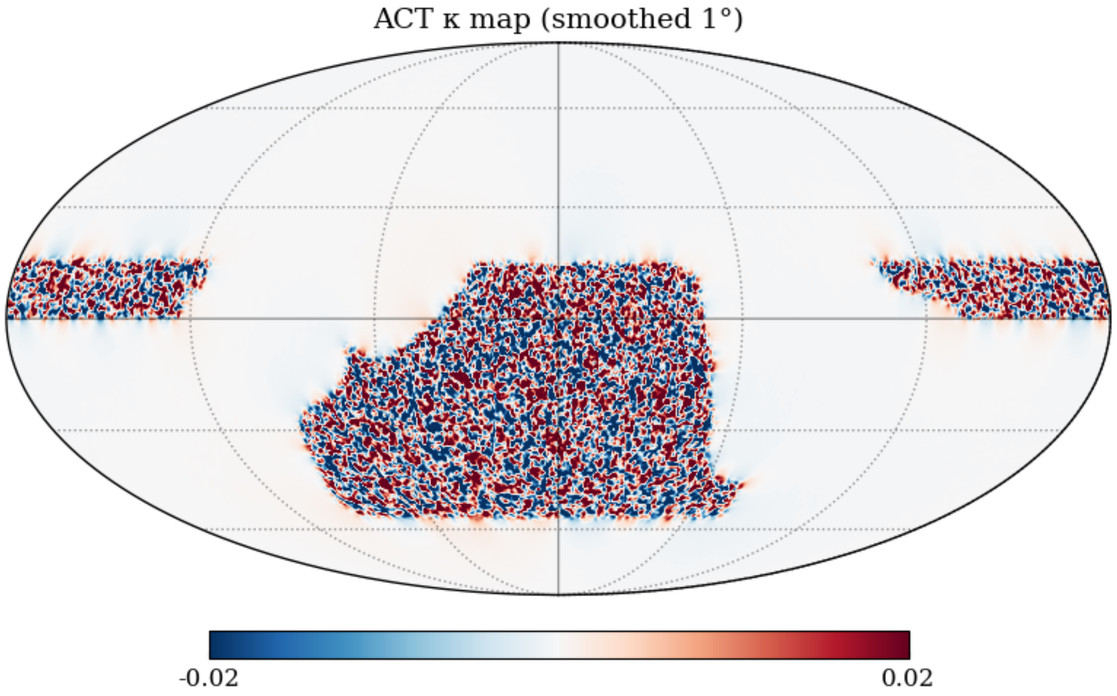
Map making – CMB lensing

We select the CMB lensing map based on the chosen field:
ACT for the South and Fornax fields, **Planck** for the North field

Planck

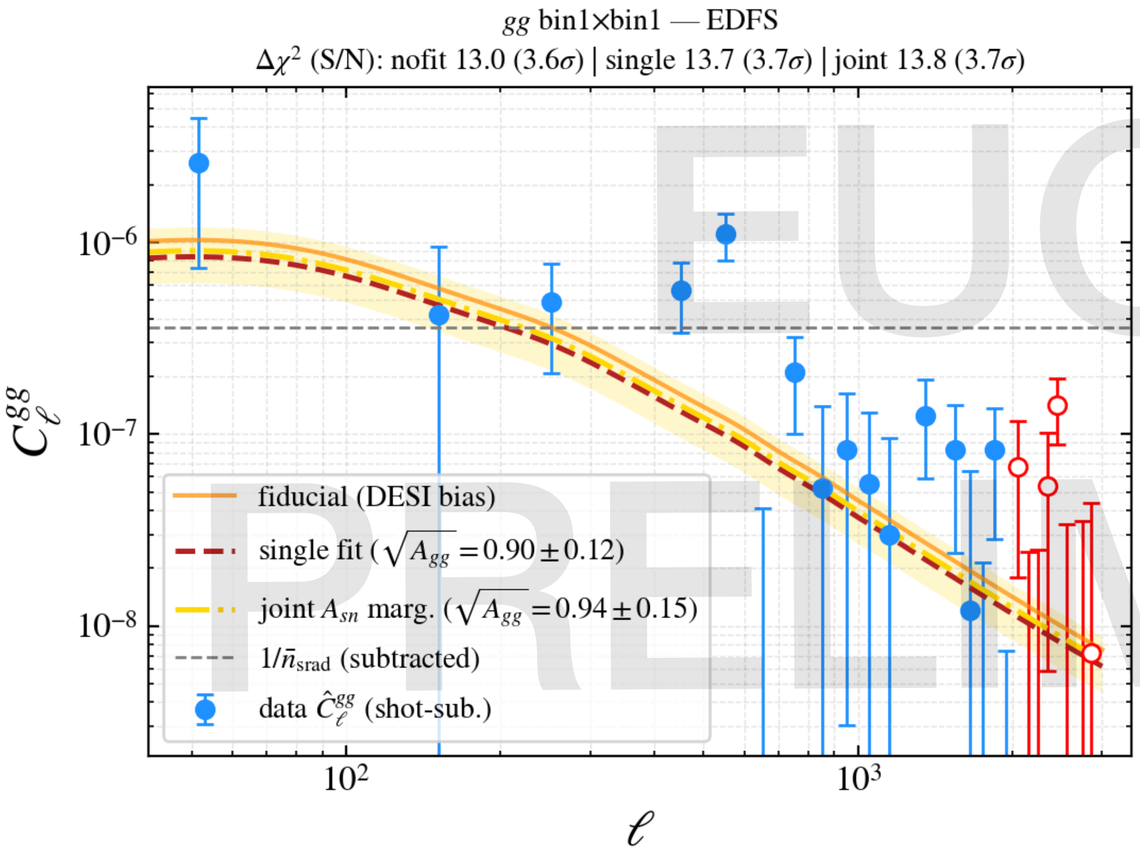


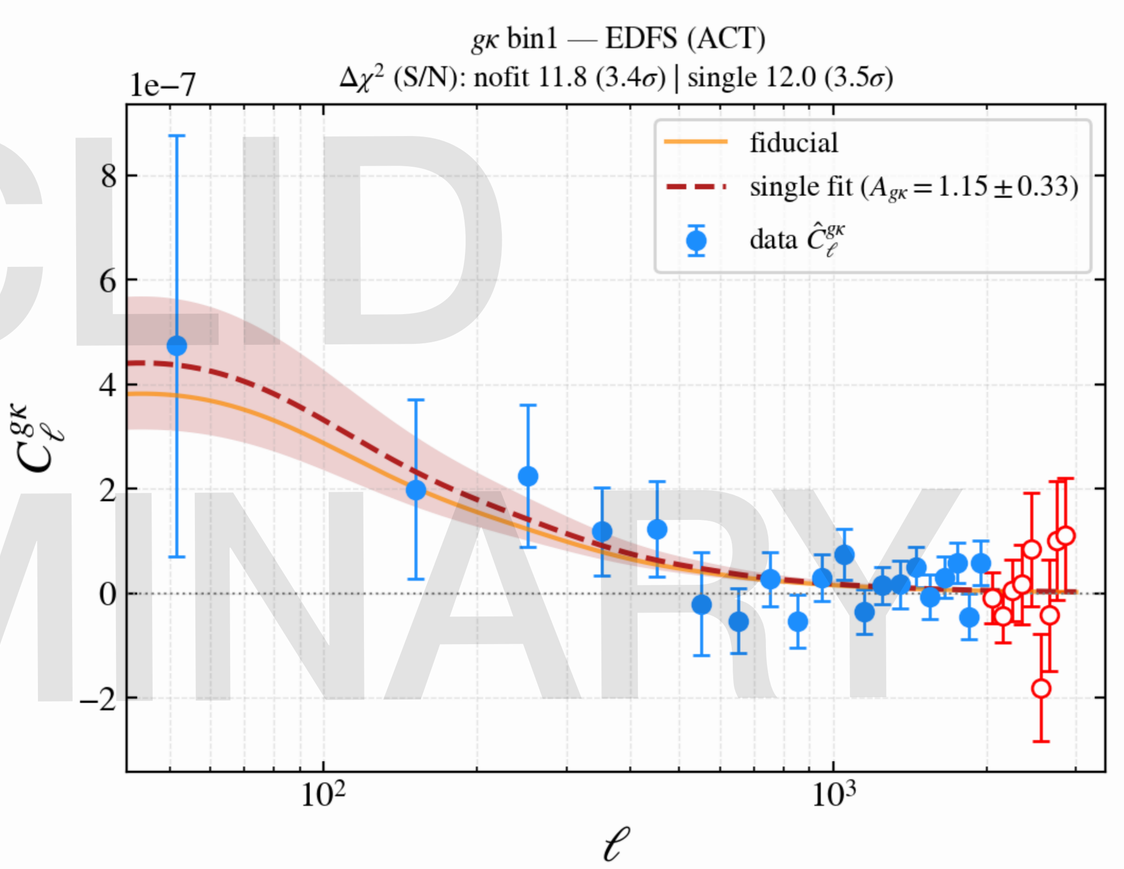
ACT



C_ℓ and Cov with NaMaster

We compute the bandpower-binned angular power spectra for $C_\ell^{\mathrm{GC}\times\mathrm{GC}}$ and $C_\ell^{\kappa\times\mathrm{GC}}$ with associated Gaussian covariance matrices for these fields



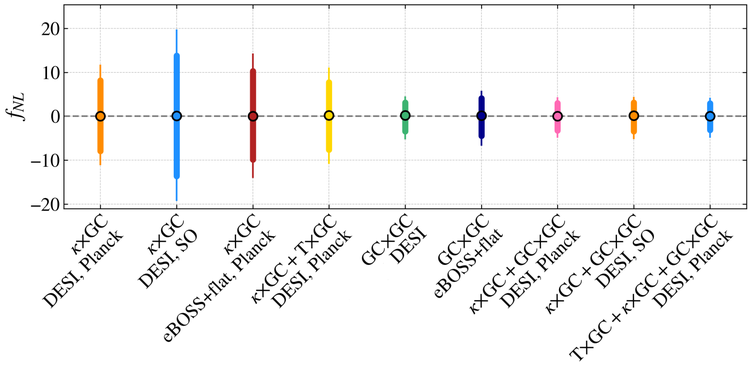


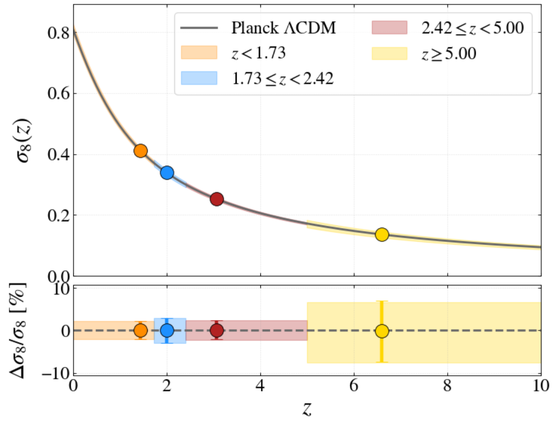
EUCLID PRELIMINARY

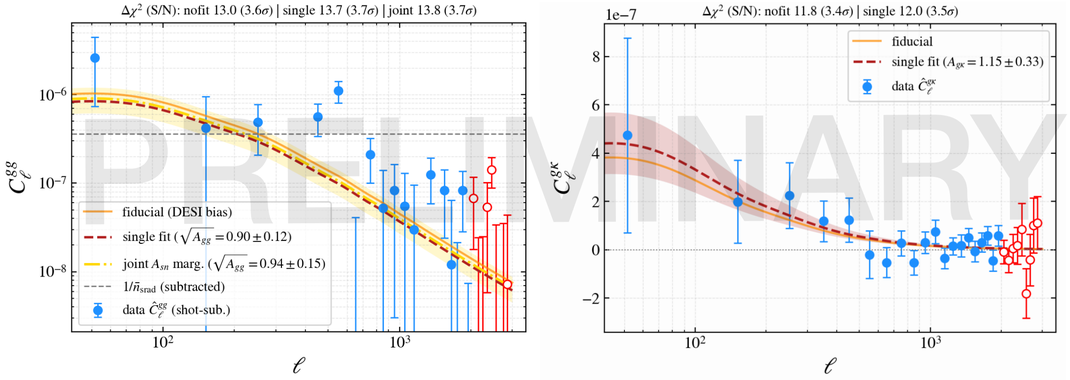
N.B. Red points are those excluded from the fit

Take-home messages and conclusions

- Euclid will observe millions of AGNs up to $z \sim 5$
- Combining AGN auto-correlation (GCxGC) and cross-correlation with CMB lensing ($\kappa \times$GC) we obtain tight measurements of PNG ($\sigma_{f_{\rm NL}} \approx 2.5$)
- Extending the "2x2pt" to "3x2pt" with the CMB lensing auto-correlation ($\kappa \times \kappa$), we obtain tight measurements of the amplitude of matter perturbation $\sigma_8(z)$ up to $z \gtrsim 6$
- Cross-correlating AGNs with CMB temperature anisotropies (TxGC), we are not able to obtain tight measurements of ISW
- Developed a pipeline for Euclid Q1 AGNs and for soon-available Euclid DR1. First Q1 measurements look promising!







PRELIMINARY

contact
matteo.peronaci@uniroma1.it

Backup slides

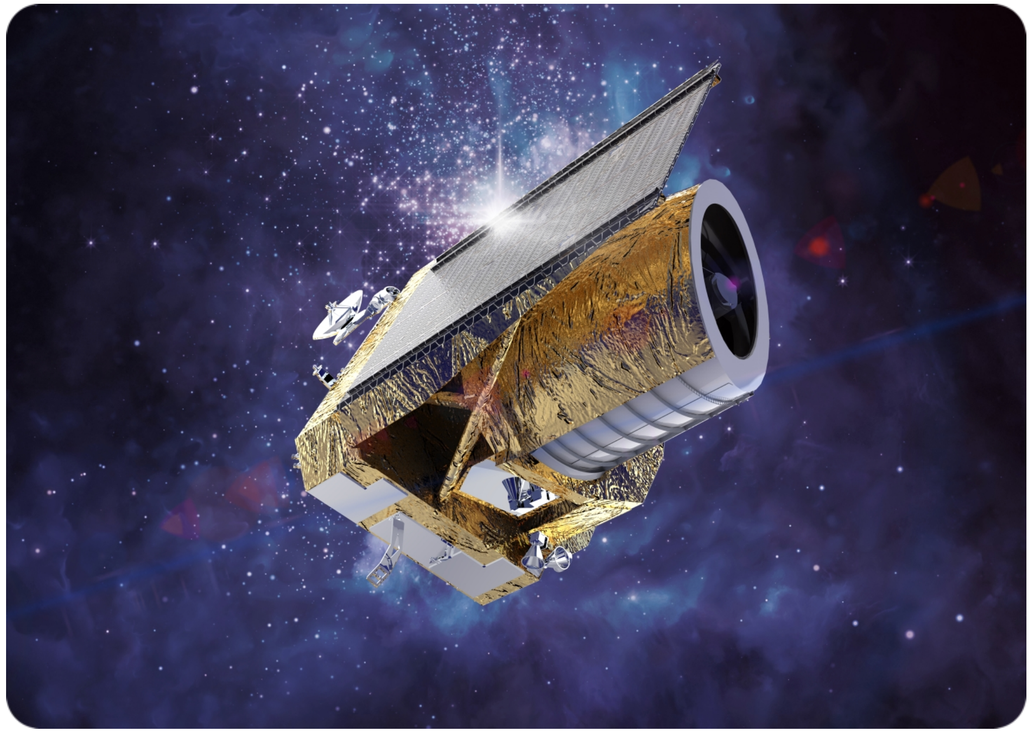
The Euclid mission: mapping the dark universe

Launched in 2023, currently collecting data from the second Lagrange point (L2)

Main objective: investigate the expansion of the universe and the nature of dark energy and dark matter

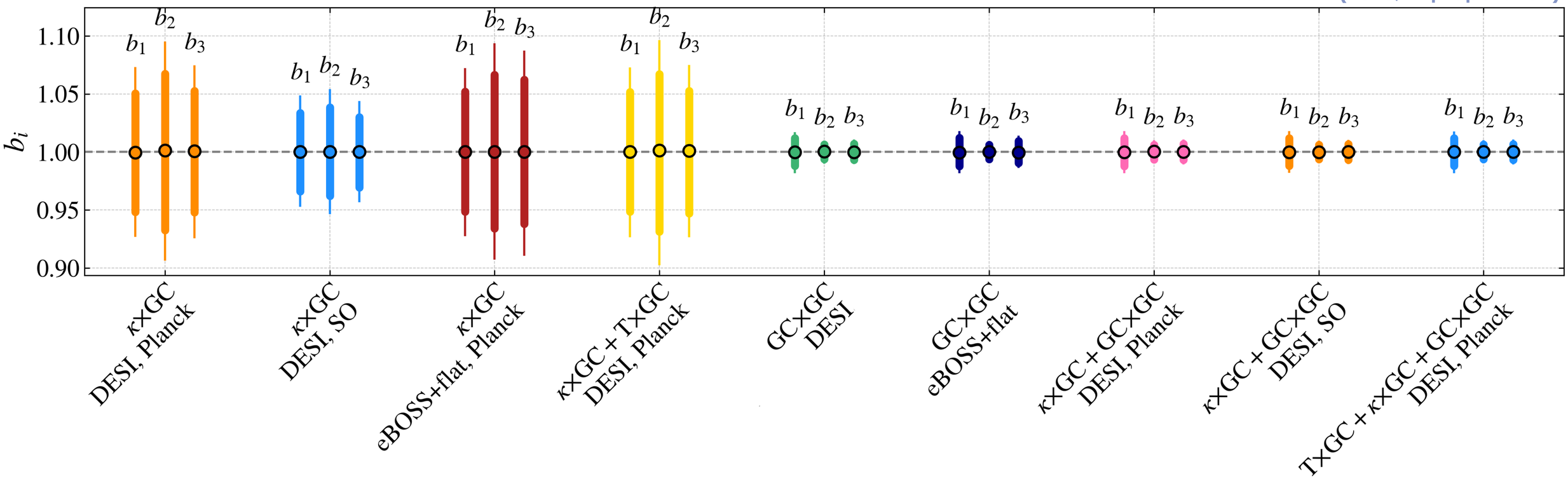
Primary probes: galaxy clustering and weak gravitational lensing

Additional observables: AGNs, high-z galaxies, supernovae, galaxy clusters, exoplanets, local observables…



Results – Primordial non-Gaussianity $f_{\rm NL}$

M. Peronaci et al. (2026, in preparation)



We will be able to improve our knowledge on AGN bias and distinguish between different bias models

N.B. "DESI", "eBOSS+flat" are the AGN bias models assumed
N.B. "Planck", "SO" are the lensing noise curves

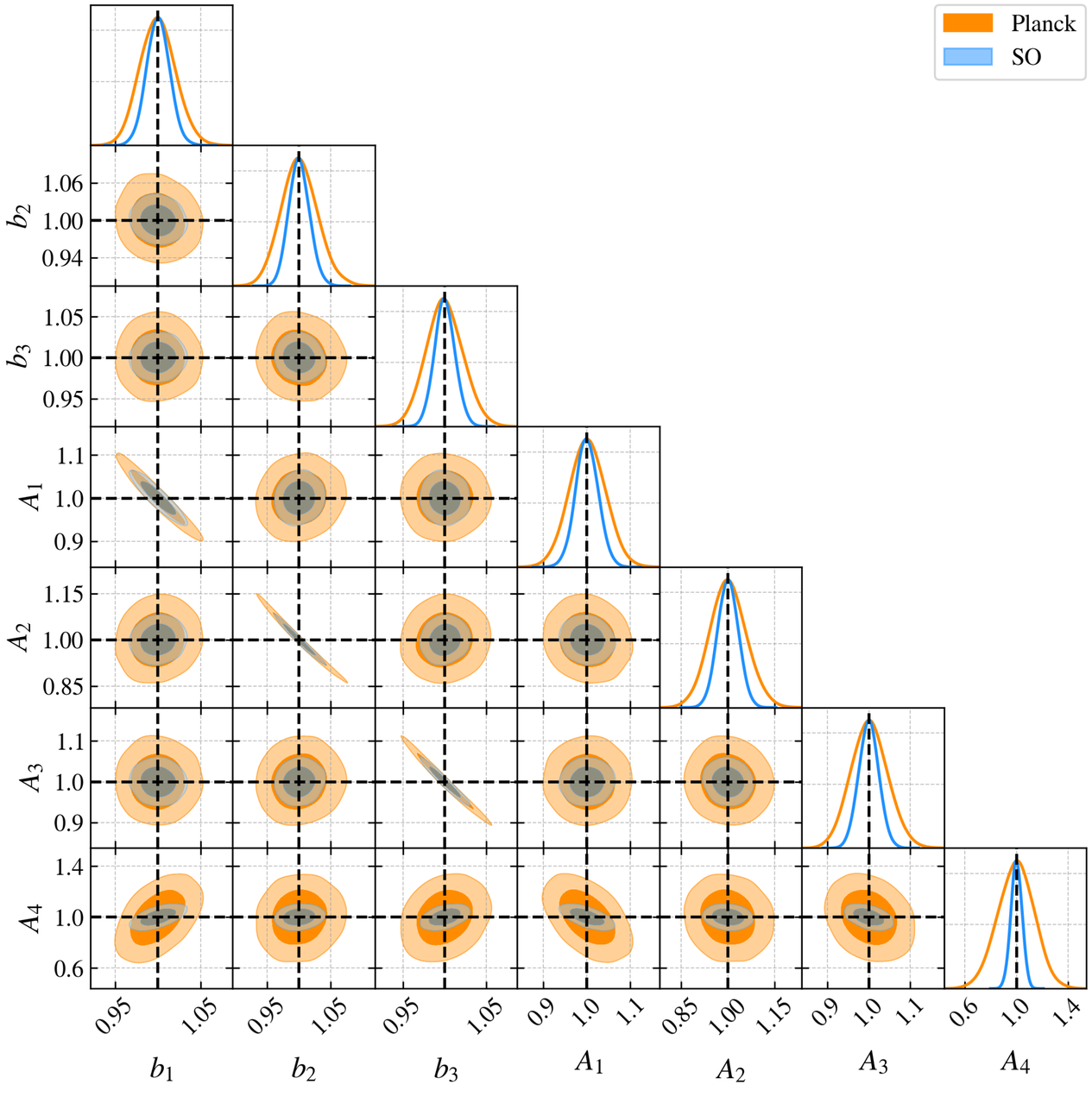
Results – Amplitude of matter perturbations $\sigma_8(z)$

The combination of $\kappa\times\kappa + \kappa\times$GC+GC$\times$GC helps us fixing A_i for each redshift interval

Once we have A_i we obtain unique measurements of structure growth at high redshifts

$$\tilde{\sigma}_8(z_i) = \sigma_8(z_i)\sqrt{A_i}$$

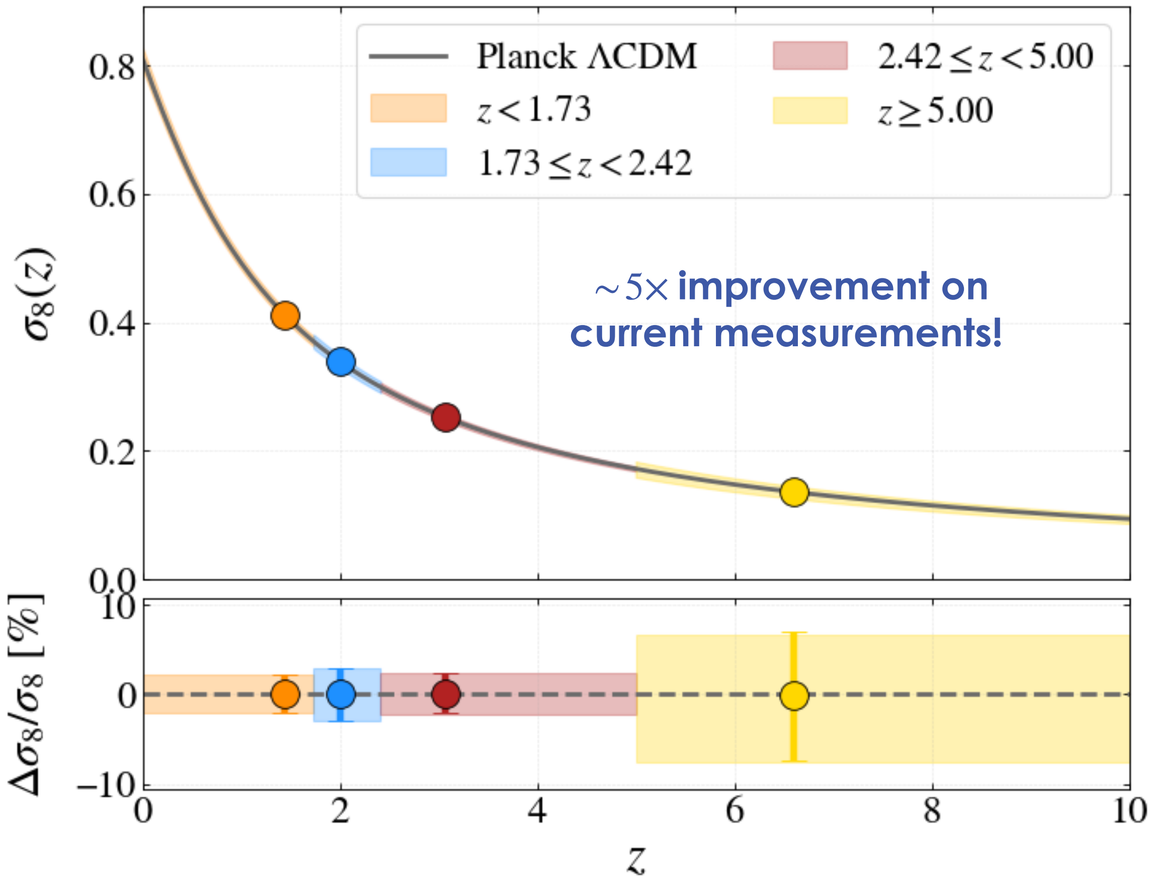
M. Peronaci et al. (2026, in preparation)



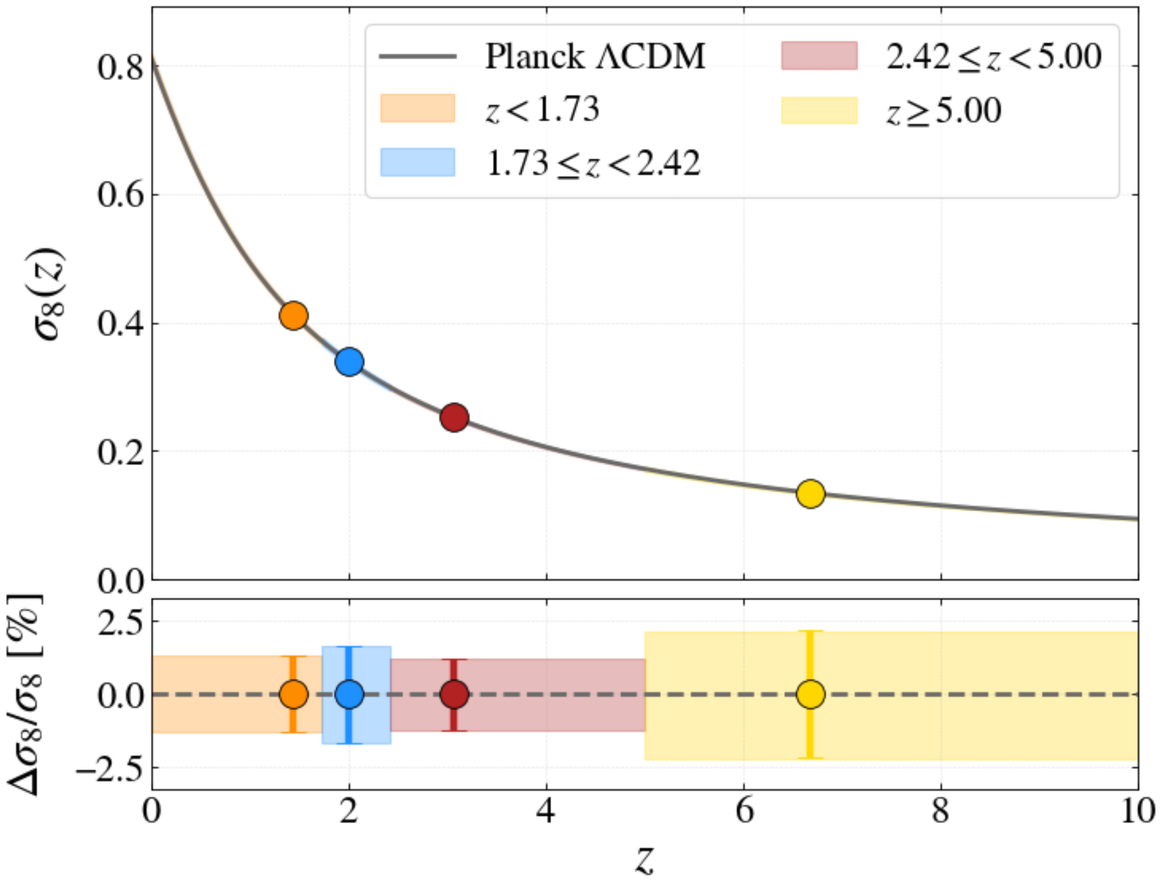
Results – Amplitude of matter perturbations $\sigma_8(z)$

The "3x2pt" combination reconstructs structure growth $\sigma_8(z)$ in four redshift intervals up to high z

Planck κ CMB



SO κ CMB



M. Peronaci et al. (2026, in preparation)

C_ℓ and Cov with NaMaster

From the AGN and CMB maps, it is possible to use Namaster to compute the pseudo-C_ℓ:

$$\tilde{C}_\ell(a_v, b_w) = \frac{1}{2\ell+1} \sum_{m=-\ell}^{\ell} a_{v,\ell m} b^{\dagger}_{w,\ell m}$$

Where a_v, b_w are the masked AGN and CMB lensing fields.

Because of the mask, the pseudo-C_ℓ is biased. Its ensemble average is a linear combination of the true, underlying power spectra $C_{\ell'}$:

$$\langle \tilde{C}_\ell \rangle = \sum_{\ell'} M_{\ell\ell'} C_{\ell'}$$

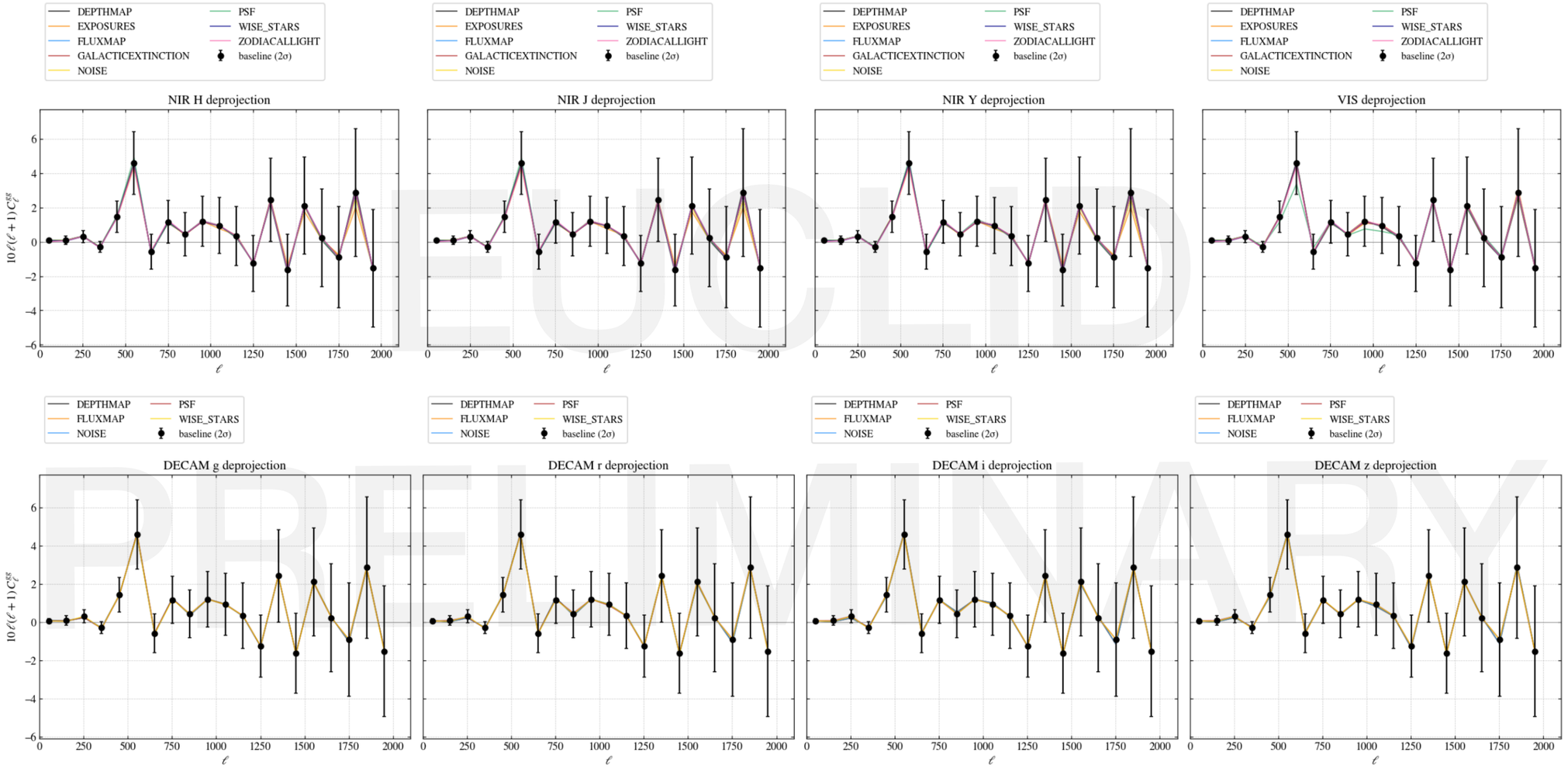
Where $M_{\ell\ell'}$ is the mode-coupling matrix. Namaster calculates it analytically based entirely on the geometry and power spectrum of the input masks.

Also, because the mask removes information, the full matrix cannot be inverted. To solve this, NaMaster groups the multiples into band powers with specific weights w^q_ℓ:

$$\tilde{B}_q = \sum_{\ell \in q} w^q_\ell \tilde{C}_\ell \Longrightarrow B_q = \sum_{q'} \left(M_{qq'} \right)^{-1} \tilde{B}_{q'}$$

Systematics deprojection

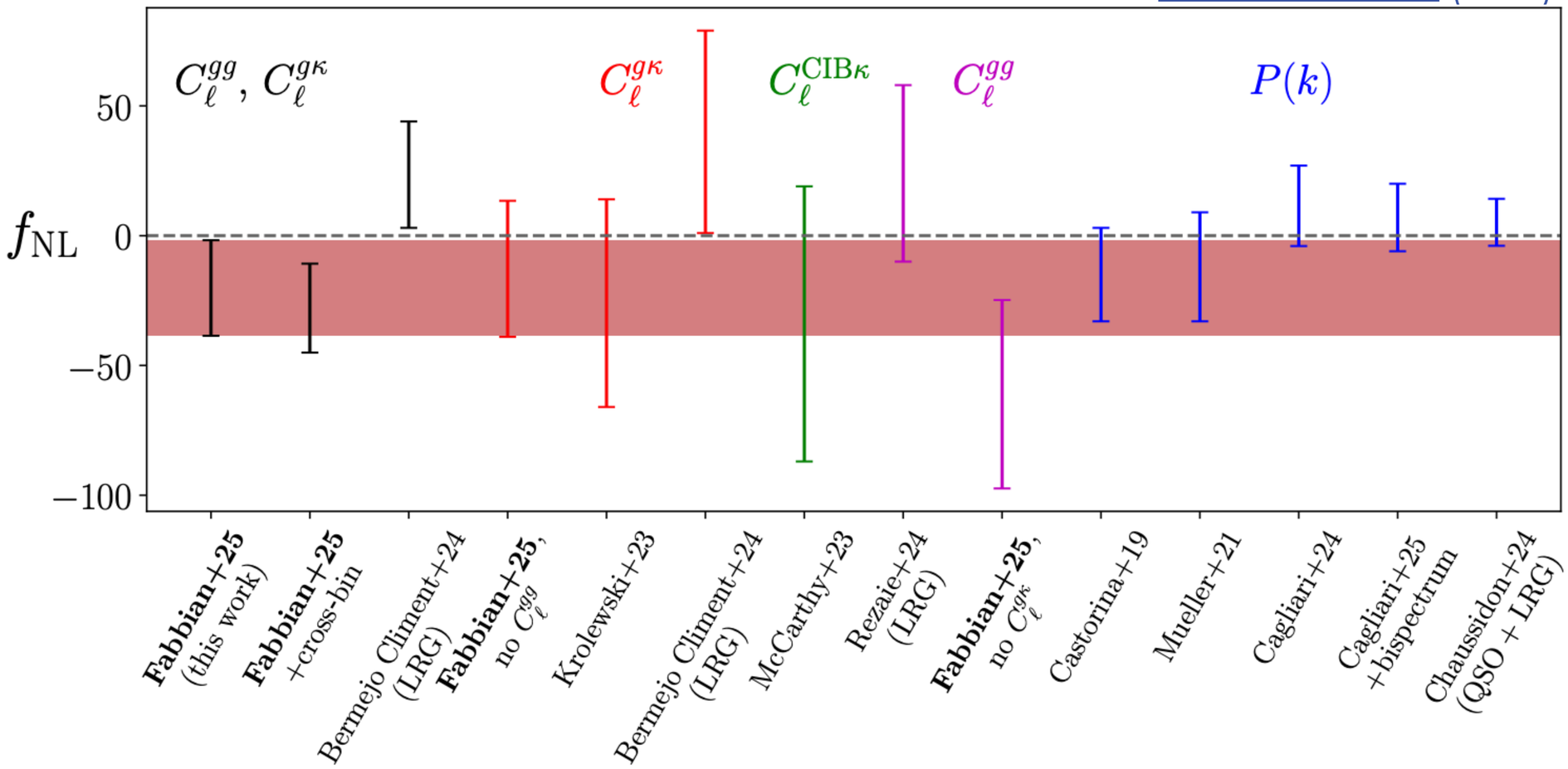
We analyse many observation templates and deprojects them to test if the measured signals are driven by observational systematics like stellar crowding or dust



EUCLID
PRELIMINARY

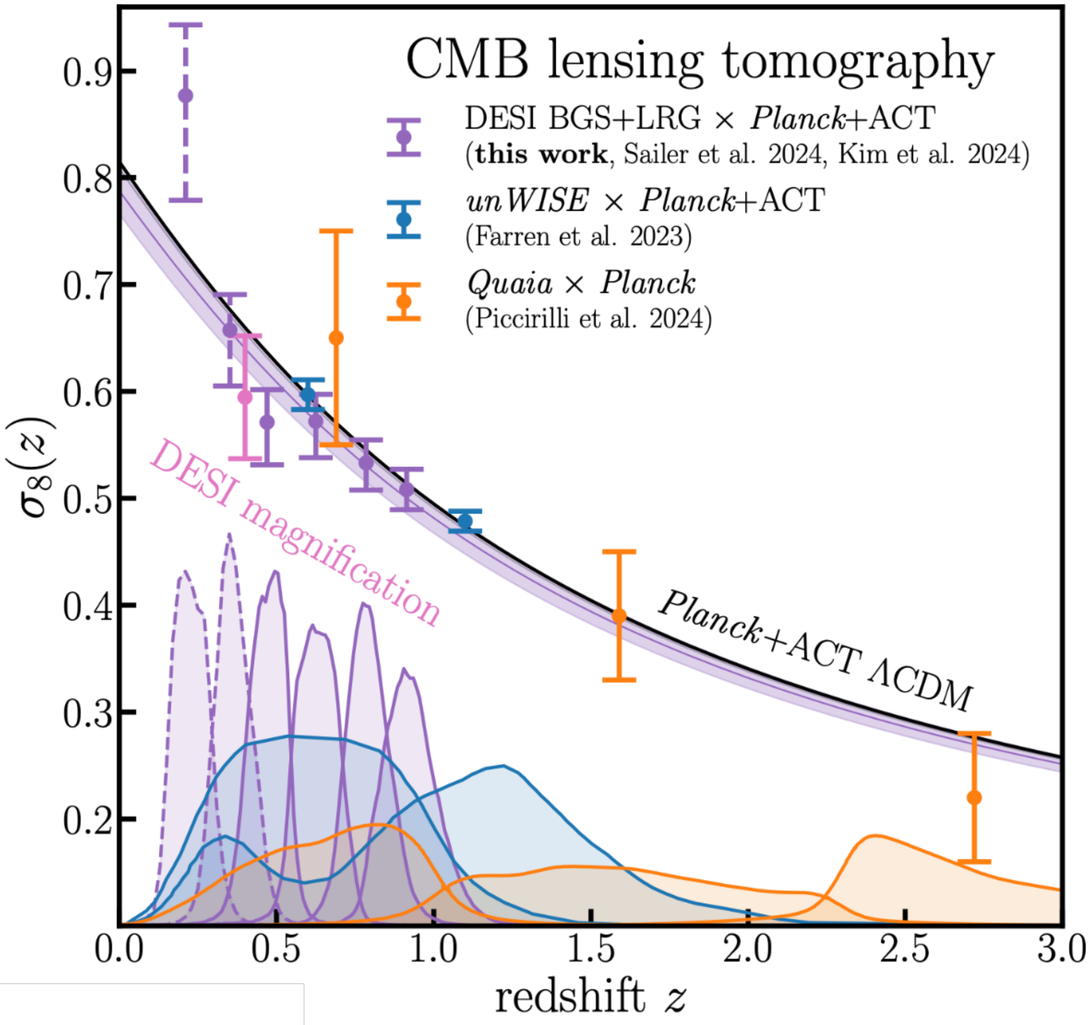
Current constraints on $f_{\rm NL}$ w/LSS

G. Fabbian et al. arXiv:2504.20992 (2025)



Current constraints on $\sigma_8(z)$ w/CC

N. Sailer et al. arXiv:2503.24385 (2025)



C. Villagra et al. arXiv:2507.08798 (2025)

